# FLOOD RISK ASSESSMENT IN KALU RIVER BASIN IN SRI LANKA USING GEOSPATIAL TECHNIQUES AND HYDROLOGICAL MODELLING

RAJESH GURUNG

(208352V)

Degree of Master of Science

Department of Civil Engineering

University of Moratuwa
Sri Lanka

February 2022

# FLOOD RISK ASSESSMENT IN KALU RIVER BASIN IN SRI LANKA USING GEOSPATIAL TECHNIQUES AND HYDROLOGICAL MODELLING

RAJESH GURUNG

(208352V)

Supervised by

Dr T. M. N. Wijayaratna

Thesis submitted in partial fulfillment of the requirements for the degree Master of Science in Civil Engineering

UNESCO Madanjeet Singh Centre for

South Asia Water Management (UMCSAWM)

Department of Civil Engineering

University of Moratuwa

Sri Lanka

February 2022

# DECLARATION OF THE CANDIDATE AND SUPERVISOR

“I declare that this is my own work and this thesis does not incorporate without acknowledgement any material previously submitted for a Degree or Diploma in any other University or institute of higher learning and to the best of my knowledge and belief it does not contain any material previously published or written by another person except where the acknowledgement is made in the text”.

Also, I hereby grant to University of Moratuwa the non-exclusive right to reproduce and distribute my thesis/dissertation, in whole or in part in print, electronic or other medium. I retain the right to use this content in whole or part in future works (such as articles or books).

UOM Verified Signature

25/01/2022

RAJESH GURUNG

Date

The above candidate has carried out research for the Masters/MPhil/PhD thesis/ Dissertation under my supervision

UOM Verified Signature

27/01/2022

Dr T. M. N. Wijayaratna

Date

# ABSTRACT


## Flood Risk Assessment in Kalu River Basin in Sri Lanka using Geospatial Techniques and Hydrological Modelling

Kalu Ganga basin is one of the main waterway basins in Sri Lanka which gets exceptionally high rainfalls with higher discharges. This report is about how the different zones, having a higher likelihood of a flood in the Kalu Ganga basin can be identified through remote sensing and geospatial approach. RRI model was additionally used to get the flood extents to verify the flood susceptibility map. Six flood influencing parameters (elevation, slope, land use, flow accumulation, soil, and rainfall) were taken for obtaining a flood susceptibility map with the AHP method in ArcMap. In the RRI model, the built-in data (Flow Direction, Flow Accumulation, DEM, Soil, and Land Cover) with observed rainfall data was used for generating a flood inundation map. The flood susceptibility map has a flood susceptibility area under the Very High category of 267 km² (8.4%) in the Kalu Ganga basin which is the most probable flood occurrence area. The flood inundation maps of May 2003, April 2008, and May 2008 have an area of 217.9 km² (6.3%), 193.6 km² (5.6%), and 108.5 km² (3.1%), respectively with flood depths greater than or equivalent to 1 meter in Kalu Ganga basin where the flood depths greater than or equivalent to 1 meter cover all the flood depths. In the AHP method, the rainfall parameter greatly influenced the flood susceptibility map. The built-in data with *nr* river value and *ns* slope values greatly influence the flood inundation map in the RRI model. The flood susceptibility map from the AHP method in ArcMap has a higher flood potential area than the flood inundation map obtained from the RRI model, and this is because the simulated or observed flood maps are always a subset of the flood susceptibility map. The flood susceptibility map obtained from the AHP method in ArcMap is a flood probability map and the flood inundation map from the RRI model is a simulated flood map. Therefore, they are different. However, the flood inundation area occurs within the flood susceptibility map. The Analytical Hierarchy Process (AHP) method is an alternative quick method of identifying flood potential areas and it can be applied to any other place around the world for the prevention and management of flood hazards.


**Keywords: Analytical Hierarchy Process (AHP), Flood Mapping, Flood Risk Analysis, Rainfall-Runoff-Inundation (RRI) Model**

# DEDICATION

This thesis is dedicated to my father R.B. Gurung and my mother Sumitra Gurung who have been the source of inspiration and gave me moral support to proceed with my higher studies.

To my brothers Robin Gurung, C.K. Gurung, and Nirmal Gurung for giving me advice and encouragement to finish my thesis. To my sister in laws Daw Dem and Tshering Zam who gave me emotional support throughout my research. To my nephews Keldhen Gurung and Gesyel Mipham Wangyel for showering me with love and happiness.

And last but not the least, I dedicate this book to almighty god, thank you for the strength, happiness, and for giving me a healthy life. All of these, I offer to you

.

# ACKNOWLEDGEMENTS

I want to pass on my true appreciation to my research supervisor, Dr. Nimal Wijayaratna for his nonstop help stretched out during the research, for his patience and guidance. Without his devoted oversight and consistent direction, this research would not have been a triumph. I am exceptionally thankful to him for his important time with me towards finishing this research.

I would like to convey my sincere gratitude to the Centre Chairman, Professor R.L.H.L Rajapakse for stretching out all the assistance to make the progress of this program. His guidance, help, and support amidst his busy schedule are greatly appreciated.

I would also like to thank Late Shri Madanjeet Singh, the Founder of SAF-Madanjeet Singh Scholarship, South Asia Foundation (SAF), the University of Moratuwa, and Organization for Youth Empowerment (SAF Bhutan Chapter) for giving me this opportunity to join this study towards a master's degree of Water Resource Engineering and Management, at UNESCO Madanjeet Singh Centre for South Asia Water Management (UMCSAWM), Department of Civil Engineering, University of Moratuwa, Sri Lanka.

My appreciation is additionally reached out to Miss Gunjan Kour, Miss Tina Sultana, Mr. Utsab Phuyal, Mr. Virendra Kumar, and Mr. Farid Farhat who gave me support to do the research successfully is greatly appreciated.

# TABLE OF CONTENTS

# LIST OF FIGURES

# LIST OF TABLES

# LIST OF ABBREVIATIONS

| | |
|---|---|
| AHP | Analytical Hierarchy Process |
| CSV | Comma-Separated Values |
| DEM | Digital Elevation Model |
| DMC | Disaster Management Centre |
| DOI | Department of Irrigation |
| GIS | Geographic Information System |
| HDX | Humanitarian Data Exchange |
| IDW | Inverse Distance Weighting |
| JICA | Japan International Cooperation Agency |
| LULC | Land Use Land Cover |
| MODIS | Moderate Resolution Imaging Spectroradiometer |
| NBRO | National Building Research Organization |
| NSC | Nash-Sutcliffe efficiency |
| OCHA | United Nations Office for the Coordination of Humanitarian Affairs |
| PDNA | Post Disaster Needs Assessment |
| $R^2$ | Coefficient of Determination |
| RF | Rainfall |
| RRI | Rainfall-Runoff Inundation |
| SF | Streamflow |
| SRTM | Shuttle Rader Topographic Mission |

# CHAPTER 1

## 1 INTRODUCTION

Flood is perhaps the most widely recognized regular hazard that happens throughout the planet except for the polar locales. Floods are one sort of catastrophe throughout the planet, influencing living souls and making monetary misfortunes. (Das, 2018). Flood inundation can be defined as an overspill of water that submerges usually dryland areas. It occurs rapidly and at times is accompanied by landslides, bridge collapse, damage to buildings, and fatalities (Hapuarachchi et al., 2011).

Almost all the countries are affected by floods, and the damage is generally high in developing countries of Asia and Africa, particularly in deltaic regions, as existing countermeasures are presently not strong enough. Therefore, flood-risk assessments in those regions are essential (Bhagabati & Kawasaki, 2017).

Sri Lanka is situated on the way of two restricting monsoon seasons causing it to receive rainfall from the monsoon over a large period of the year. Inter-monsoon rainfall additionally brings downpours over a large part of the balance period reducing the dry seasons to a few months in Sri Lanka. This monsoon pattern, with occasional cyclones, makes much of the island susceptible to floods. Floods have happened over a significant part of the year in Sri Lanka, except during the driest months.

Although very few places in Sri Lanka can be said to be free from flooding, most of the areas are prone to floods. Kalu Ganga river flowing to the sea on the western coast is highly exposed to frequent floods. In addition, most of the rivers originating from the central highlands are vulnerable to flooding in the valleys.

Kalu Ganga basin is the second largest basin in Sri Lanka and perhaps the main waterway basin in Sri Lanka which gets exceptionally high rainfalls and has higher discharges. Because of its hydrological and geographical characteristics, the lower floodplain experiences regular floods, drastically affecting the economy. (Ampitiyawatta & Guo, 2010).

Frequent flooding along Kalu Ganga is a persistent event that people living around the banks of Kalu Ganga river, and its tributaries experience every year. The floods occur due to the high amount of rainfall in the catchment area and the gradient differences of the river. The gradient is very low downstream of Rathnapura to the upper stream of Kalutara town. This low gradient is inadequate to provide sufficient velocity for the water to move downstream. The narrow gap or the bottleneck in the Ellagawa area of the river retains the water for many days in the Ratnapura District before it is discharged to Kalutara District. Sand extraction has deepened the river and has helped to reduce the flood to a certain extent, but the lack of proper flood mitigation infrastructures is still a major cause of floods in the Kalu river basin (Ampitiyawatta & Guo, 2010).

Flood mapping is important for flood risk management and risk reduction. Flood mapping helps to reduce the loss and damage caused by floods. If the areas having high exposure to flood risk is known, then it will be easy to decide not to build infrastructure there. Flood maps also play an important role in risk communication, if people know that they live in a high flood risk area then they will seek information on how to protect themselves and take alerts and warnings seriously.

At present times, remote detecting and the geographic data framework are extensive tools for the evaluation of hydrological investigation. These tools are capable to provide quite an accurate output in a cost- and time-effective manner (Das, 2018).

The combination of the AHP and GIS techniques contributes a dynamic tool for decision-making procedures for flood hazard mapping, as it provides a logical and efficient use of spatial data. The use of multi-criteria evaluation for different factors is also demonstrated to be useful in the definition of the risk areas for flood mapping and possible prediction. Overall, the GIS-AHP based category model is effective in flood risk zonation (Ouma & Tateishi, 2014).

This report shows how the different zones that have a higher likelihood to flood in the Kalu Ganga basin could be easily identified through remote detecting and geospatial approach. The Analytical Hierarchy Process (AHP) approach was used to generate a flood susceptibility or probability map. Further, the Rainfall-Runoff-Inundation (RRI) model was used to develop flood inundation regions to verify the AHP flood susceptibility maps.

A total of six influencing factors, such as elevation, slope, rainfall, flow accumulation, land use, and soil were evaluated individually as well as combined with GIS software by providing relative weights through the Analytical Hierarchy Process (AHP) approach. In the RRI model, the built-in grided data (Flow Direction, Flow Accumulation, DEM, Soil, and Land Cover) along with observed precipitation data were used.

The flood susceptibility map obtained from the AHP method in ArcMap is a flood probability map and the flood inundation map from the RRI model is a simulated flood map. Therefore, they are different. However, the flood inundation area occurs within the flood susceptibility map. The flood susceptibility map developed through the AHP is always the maximum extent that an actual flood map can extent. The AHP method is an easy alternative to flood mapping through observations or flood modeling and it can be applied to any other place around the world for the prevention and management of flood hazards.

## 1.1 Problem Statement

Kalu Ganga basin is a highly populated area consisting of metropolitan areas and agrarian fields. River floods frequently occur in this area resulting in severe damage and destruction. Local planners, decision-makers, and disaster relief organizations lack accurate information on the spatial appropriation of flooding. Flood relief and mitigation planning are at a minimal level demanding immediate concern in the Kalu Ganga basin (Peiris et al., 2009). There is a lack of accurate information on flood mapping in the Kalu Ganga basin which includes the flood-prone zones.

## 1.2 Objective

To generate a flood susceptibility map in the Kalu Ganga basin using geospatial techniques with Analytical Hierarchy Process (AHP) and developing flood inundation map with Rainfall-Runoff Inundation (RRI) Model.

## 1.3 Specific Objective

- To generate flood susceptibility map by overlaying of pre-processed maps using AHP Method with ArcMap.
- To generate flood inundation map using RRI Model.
- To verify the precision of the flood susceptibility map produced from the AHP method in ArcMap and by using the flood inundation maps generated from the RRI Model.

## 1.4 Significance of the Research

- This case study will help to identify flood sensitive areas in the Kalu Ganga basin
- This case study will help to identify the maximum flood extents in the Kalu Ganga basin.
- The outcome of this research can be useful for researchers, planners, and managers to manage the vulnerable areas to flood and reduce damages.
- The flood susceptibility map can be used for flood mitigation, evacuation during the flood, preventing adverse effects and for insurance schemes in flood-prone areas.

## 1.5 Study Area

Kalu Ganga basin located in Sri Lanka has an area of 3,191 km$^2$. Kalu river flows through Kalu Ganga Basin and it has a length of 129 km. It is in the wet climatic zone. The Kalu river has its origin in Sri Padaya (elevation 2,400 meters) and the sea outlet in Kalutara. The average annual rainfall in Kalu Ganga Basin is in the range of 2,000 – 6,000 mm.

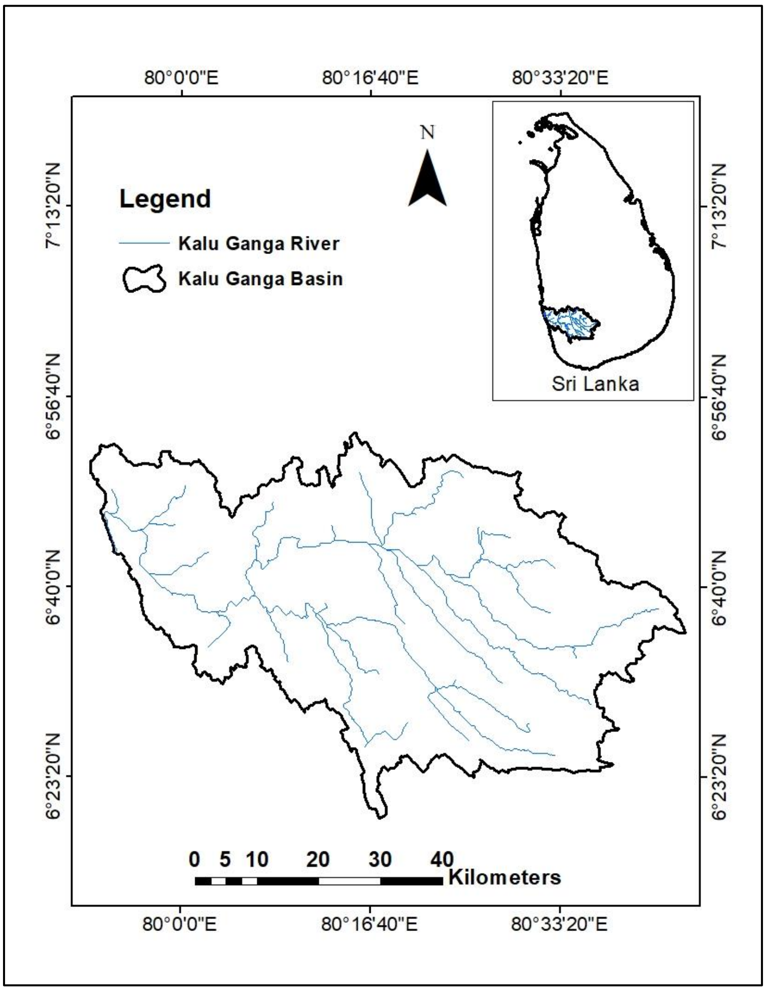


Figure 1-1: Study Area

(*Source: SRTM, Resolution 90 m*)

# CHAPTER 2

## 2 LITERATURE REVIEW

The first few sections of the literature review are about the flooding in the Kalu river which covers the information of historical floods in the Kalu River. It is then followed by a section on hydrological data preparation such as accuracy checking and filling the missing rainfall and stream data.

The literature review then focused on Analytical Hierarchy (AHP) Method and Rainfall-Runoff-Inundation (RRI) Model. Under the section on the AHP method, the research work carried out on parameters taken for the AHP method, the Inverse Distance Weighting interpolator (IDW) method for rainfall distribution map, and the AHP procedure to generate the flood susceptibility map were critically appraised. Under the RRI model, the studies done on the parameters taken in the RRI model, and the objective functions taken for model calibration and validation are discussed.

### 2.1 Flooding in Kalu River

The Kalu river, starting from the central hills of Sri Lanka, flows down from Ratnapura and Horana and discharges into the Indian Ocean at the outlet Kalutara. Between the origin of the river and Ratnapura town, the flow stretch is described by a narrow bed and huge banks on both sides before it enters the Ratnapura town. Ratnapura region is generally vulnerable to floods due to the Kalu River and its tributaries. Severe floods categorized as major floods (flood levels above 24.4 m ASL at Ratnapura, stated by DOI) occurred in the years 1913, 1940, 1941, 1947, and 2003. The flooding of May 2003 in the Kalu Ganga basin was the severest in terms of flood impact (JICA, 2009).

A feasibility study on flood prevention of the Kalu Ganga basin and a feasibility study for a multipurpose Ratnapura Dam for flood prevention and hydropower generation was carried out by TAHAL Group (2013). It included the development of the SOBEK model, field examination, and tender documentation for flood mitigation measures.

Kalutara city is located at the river outlet of the Kalu river, its development area stretches along the river. Ratnapura city, on the other hand, is a commercial development center of the central part of the Island. Ratnapura's new urban development plan has been formed and further development is expected. Public and commercial centers are planned in such a way that it is separated from the existing town center, which is regularly affected by flooding. The river conservation area along the Kalu river is demarcated, which will be an important approach for flood prevention and management in this area (JICA, 2009). Local planners, decision-makers, and disaster relief organizations lack accurate information on the spatial appropriation of flooding. Flood relief and mitigation planning are at a minimal level demanding immediate concern in the Kalu Ganga basin (Peiris et al., 2009). This report produces a flood susceptibility map that can be used for flood relief and mitigation planning in the Kalu Ganga basin. It can be used to identify flood-sensitive areas and for studying future scenarios of flood-prone areas. However, the validation of flood susceptibility extent with a satellite flood map is difficult since the flood map from the AHP is a probability map without a particular return period showing areas with different potentials for flooding.

## 2.2 Data Preparation

Rainfall data were collected for eleven rainfall stations (1970-2015). Rainfall data from eleven stations were used since the study area covers a very huge area. While carrying out visual checking for rainfall data, missing rainfall data were found. It is important to fill the missing rainfall data and check for accuracy since the rainfall distribution map obtained from the IDW method in ArcMap, used in the AHP method to generate flood susceptibility map, is sensitive to the rainfall data used.

Subramany (2019) proposed when the missing rainfall data that is the annual average rainfall difference between the two stations is less than 10%, then a simple arithmetic average procedure is followed to estimate the missing rainfall values. If the difference is greater than 10%, the normal ratio method is used (Subramany, 2019). The single mass curve and double mass curve were plotted after filling the missing rainfall data to check the consistency of the rainfall data.

The missing streamflow data were filled by the simple arithmetic average procedure. The rainfall versus streamflow graph was plotted to check the rainfall and streamflow data.

## 2.3 Analytical Hierarchy Process (AHP)

The analytical hierarchy process (AHP) is a technique for organizing and analysis of complicated decisions, based on mathematics and psychology. This technique was created by Saaty during the 1970s. It deals with a precise way to evaluate the weights of choice measures. Inputs from professionals are used to examine the overall sizes of variables through pair-wise evaluation. The relative importance of each pair is compared using a specially designed questionnaire (Ouma & Tateishi, 2014). The analytical hierarchy process is an amazingly stretchy and all-around coordinated approach that can interpret complicated decision issues where multiple factors are involved (Saaty, 1980).

The AHP is most helpful when finding choices to complex issues with high stakes. It stands apart from other dynamic strategies as it evaluates models and choices that customarily are hard to quantify with hard numbers. Rather than endorsing a "right" choice, AHP benefits decision-makers to observe one that best suits the qualities and the comprehension of the issue. The AHP method enjoys interesting benefits when significant components of the choice are hard to evaluate or think about. In addition, utilizing the AHP helps assurance as everybody feels their voices are heard, and they can eventually see how a choice was made (Saaty, 1987).

In engineering applications, the ultimate decision depends on the assessment of a set of alternatives in terms of diverse decision criteria. At times, it may be a demanding task and the Analytic Hierarchy Process (AHP) seems to provide an adequate way for accurately quantifying the applicable data (Triantaphyllou & Mann, 1995). The AHP method can be used to achieve greater consistency in the evaluations (Bernasconi et al., 2009).

### 2.3.1 DEM Data for Analytical Hierarchy Process (AHP)

The 90 m resolution Digital Elevation Model (DEM) from Shuttle Rader Topographic Mission (SRTM) was utilized in this research. ArcMap 10.3 software was used to delineate the Kalu Ganga basin, generating an elevation map, and slope map from the 90 m DEM obtained from SRTM. The flow accumulation map was obtained using tools in ArcMap (Das, 2018). The soil map (1998) and LULC map (1999) obtained from the Survey Department were used for soil classification and land use classification map, respectively. The rainfall data from 11 gauging stations with a 45-year duration (data period 1970-2015) was used. The average rainfall of 45 years was prepared in Microsoft Excel software and used for obtaining the rainfall distribution map in ArcMap using the IDW method.

After preparing the pre-processed maps, all the maps were converted to a raster format with a 90 m resolution. From there on, the raster files were reclassified using AHP ranks (Das, 2018).

### 2.3.2 IDW Method for Rainfall Distribution Map

Rainfall data is used to make a rainfall distribution map for the classification and map overlaying in the AHP method. The study area covers a huge area with a huge dataset, therefore, the IDW method which is suitable for a huge dataset is used for obtaining a rainfall distribution map.

The Inverse Distance Weighting interpolator presumes that each information point has a nearby impact that reduces with distance. Utilization of this strategy accepts the variable being planned reductions in impact with distance from its inspected area (Acharya & Singh, 2018).

IWD can assess outrageous changes in territory, for example, bluffs and separation points. Thick uniformly space focuses are very much added (level regions with precipices). IWD can increase or decrease the measure of the test focusing to impact cell values (Acharya & Singh, 2018).

IDW can deliver a pinpoint center outcome around information areas. In contrast to other addition strategies, for example, Kriging, IDW doesn't make unequivocal presumptions about the factual properties of the information. IDW is regularly utilized when the info information doesn't meet the measurable presumptions of further developed insertion techniques. This strategy is appropriate to be utilized with extremely huge info datasets (Acharya & Singh, 2018).

### 2.3.3 Analytical Hierarchy Process (AHP) Procedure

The AHP method in this research contains two sections. The first section is the main characterization plan of the relative multitude of parameters whereas indicated by the significance of all parameters are given and weights are determined. The second section is built by sorting each of the parameters into a subcategory (Das, 2018).

A pairwise comparison matrix was built. The general significance of this load of parameters was given dependent on various standards and qualities [(1) Equal Importance, (3) Moderate Importance, (5) Strong Importance, (7) Very Strong Importance, (9) Extreme Importance, and (2, 4, 6, and 8) Intermediate Values)] (Saaty, 1987). The value in the pairwise matrix was normalized to obtain the normalized values in the standard pairwise examination matrix. The consistency check was carried out using the Saaty method. All parameters considered in this review were evaluated separately and arranged into various subcategories. Various positions were given to each subcategory through relative scoring utilizing the AHP technique (Das, 2018). The weights of the parameters and ranks of the subcategories were put in the ArcMap using the weighted sum function to obtain the flood susceptibility map. The final map was categorized into four (4) classes (Low, Moderate, High, and Very High). The flood susceptibility map obtained from the AHP method was verified using the satellite flood maps.

## 2.4 Rainfall-Runoff-Inundation (RRI) Model

Rainfall-Runoff-Inundation (RRI) model is a two-dimensional model fit for re-enacting precipitation spillover and flood immersion at the same time. RRI model has default grided data that are built-in (flow direction, flow accumulation, DEM, Soil, and Land Cover) (Sayama et al., 2012).

The RRI model can recreate surface and sub-surface streams. The surface stream is determined utilizing 1-D and 2-D diffusive wave models as represented in Figure 2-1. Vertical penetration is approximated utilizing the Green-Ampt Model while the sidelong sub-surface stream is viewed as utilizing release pressure-driven inclination. A flood recipe dependent on the stream level and levee stature are utilized to assess the stream in between the waterway and the catchment (Sayama et al., 2012).

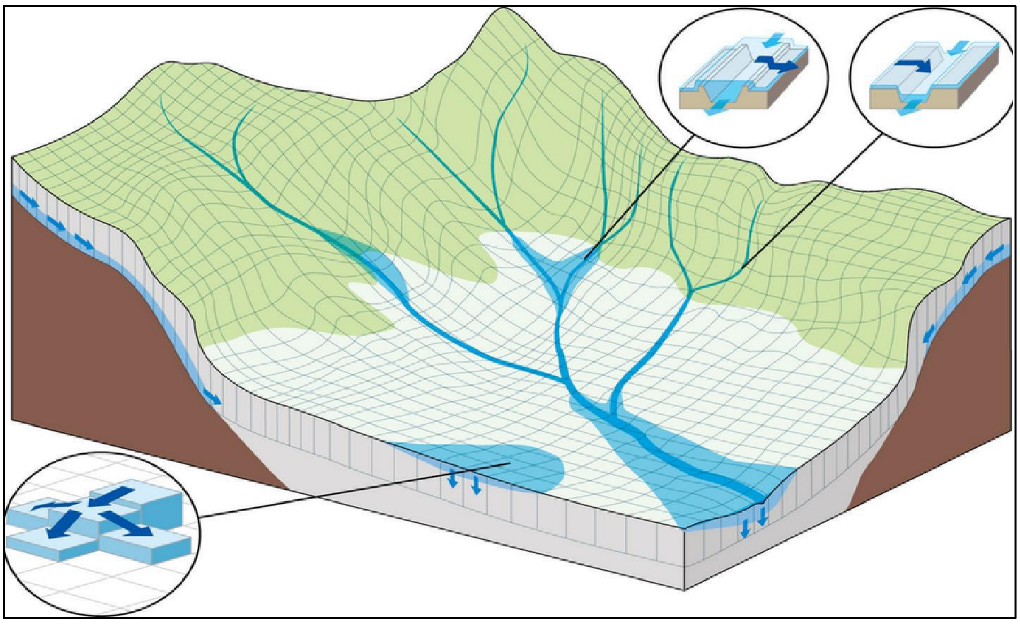

Figure 2-1: Schematic diagram of Rainfall-Runoff-Inundation (RRI) Model

(*Source:* Sayama et al., 2012)

The governing equation of the RRI model is the mass balance equation based on the continuity equation as equation [2-1]. For the unsteady flow, the momentum equation is incorporated in the governing equation in the x-direction as equation [2-2] and the y-direction as equation [2-3].

$$\frac{\partial h}{\partial t} + \frac{\delta qx}{\delta x} + \frac{\partial qy}{\partial y} = r - f \qquad [2\text{-}1]$$

$$\frac{\partial qx}{\partial t} + \frac{\partial uqx}{\partial x} + \frac{\partial vqx}{\partial y} = -gh\frac{\partial H}{\partial x} - \frac{\tau x}{\rho w} \qquad [2\text{-}2]$$

$$\frac{\partial qy}{\partial t} + \frac{\partial uqy}{\partial x} + \frac{\partial vqy}{\partial y} = -gh\frac{\partial H}{\partial y} - \frac{\tau y}{\rho w} \qquad [2\text{-}3]$$

where $h$ is water height in local surface, $t$ is time step, $q_x$ and $q_y$ is discharged per unit width in $x$ and $y$ directions, $r$ is rainfall intensity, $f$ is infiltration, $H$ is the height of the water from a datum, $u$, and $v$ are flow velocities in $x$ and $y$ directions, $\rho_w$ is the density of water, $g$ is gravitational acceleration, and $\tau_x$ and $\tau_y$ are shear stress in $x$ and $y$ directions (Onjira & Sayama, 2014).

The built-in grided data (flow direction, flow accumulation, DEM, Soil, and Land Cover) was used in this study. Ground gauge rainfall data was prepared as the input data (CSV format) and the RRI Model automatically convert it into Thiessen polygon. The output results of this model are inundation extent, floodwater depth, and river discharge. The model calibration and validation were carried out using the event-based method with observed flood levels.

### 2.4.1 Parameters for Rainfall-Runoff-Inundation (RRI) Model

The important model parameters of the RRI model are the roughness coefficient of the river channel (*nr* river) and the roughness coefficient in the river basin (*ns* slope) (San et al., 2020). By trial and error, the suitable values of *nr* river and *ns* slope are found to obtain suitable objective function values for model calibration and validation in the RRI model. The *nr* river value was taken in the range from 0.015 to 0.04 $m^{-1/3}s$ and the *ns* slope value was taken in the range from 0.15 to 1 $m^{-1/3}s$ (Abdel et al., 2018). Manning's roughness coefficient indicates the resistance to flood in channels and floodplains. Manning's roughness coefficient value (*n*) is obtained from the values of the factors that influence the roughness of channels and floodplains. (Arcement et al., 1989).

### 2.4.2 Objective Function

Hydrological models are aligned by contrasting the model re-enacted result and the observed data. In this study, the observed flood level was used for model calibration and validation. The objective function is a capacity to coordinate with the model outcome with the real world (Rabunal et al., 2009). Two objective functions, Nash-Sutcliffe efficiency (NSE) and Coefficient of Determination ($R^2$) were taken for model calibration and validation (Khaing et al., 2019).

#### *2.4.2.1 Nash-Sutcliffe Efficiency (NSE)*

Nash-Sutcliffe efficiency (NSE) demonstrates how accurately the plot of noticed versus reproduced information fits the 1:1 line (Abdel et al., 2018). According to Moriasi et al. (2015), NSE greater than 0.8 is a Very Good fit, NSE equal to 0.7 to 0.8 is a Good fit, NSE equal to 0.5 to 0.7 is a Satisfactory fit, and NSE less than 0.5 is an Unsatisfactory fit.

The NSE is given by,

$$NSC = 1 - \left(\sum_{i=1}^{N}(S_i - O_i)^2 / \sum_{i=1}^{N}(O_i - O_{mean})^2\right) \qquad [2\text{-}4]$$

where $S_i$ = model reproduced yield; $O_i$ = noticed hydrologic variable; $O_{mean}$ = mean of the perceptions that the NSE utilizes as a benchmark against which execution of the hydrologic model is looked at, and N = the absolute number of perceptions.

#### *2.4.2.2 Coefficient of Determination (R²)*

Coefficient of Determination ($R^2$) portrays the level of collinearity among mimicked and estimated information (Abdel et al., 2018). According to Moriasi et al. (2015), $R^2$ greater than 0.85 is a Very Good fit, $R^2$ equal to 0.75 to 0.85 is a Good fit, $R^2$ equal to 0.6 to 0.75 is a Satisfactory fit, and $R^2$ less than 0.6 is an Unsatisfactory fit.

The $R^2$ is given by,

$$R^2 = \frac{\left(\sum_1^n (Obs_i - \overline{obs})\,(Sim_i - \overline{sim})\right)^2}{\sum_1^n (Obs_i - \overline{obs})^2\,\sum_1^n (Sim_i - \overline{sim})^2} \qquad [2\text{-}5]$$

where $Obs_i$ is the noticed value, $\overline{obs}$ is the mean of the noticed value while $Sim_i$ is the mimicked esteem and $\overline{sim}$ is the mean of the reproduced esteem.

### 2.5 Moderate Resolution Imaging Spectroradiometer (MODIS)

The Moderate Resolution Imaging Spectroradiometer (MODIS) is a satellite sensor utilized for the earth and environment estimations. There are two (2) MODIS sensors in Earth Orbit, Terra (EOS AM) satellite, launched in 1999 by NASA, and the Aqua (EOS PM) satellite, launched in 2002. The MODIS sensor was built by Santa Barbara Remote Sensing. The data is in 36 spectral bands in varying wavelengths (0.4 μm to 14.4 μm) and varying spatial resolutions (2 bands at 250 m, 5 bands at 500 m, and 29 bands at 1 km). The sensor captures the image of the entire earth every one (1) to two (2) days. The sensor is intended to give estimations in huge scope worldwide elements including changes for earth's cover, solar radiation budget, and processes happening in the seas, and the lower atmosphere (Onjira & Sayama, 2014).

The MODIS image was downloaded from Earth data from NASA (https://earthdata.nasa.gov/). The cloud cover was identified using band 3 of the MODIS images and the cloud areas were removed (Onjira & Sayama, 2014). The threshold value of the flood area was identified and used for generating the flood area. The MODIS image was used to validate the event-based RRI model flood inundation extent.

# CHAPTER 3

## 3 METHODOLOGY

The methodology flowchart consists of two parts. The first part is the AHP method and the second part is the RRI model. Figure 3-1 shows the methodology followed in this report to obtain the flood susceptibility map from the AHP method and flood inundation maps from the RRI model.

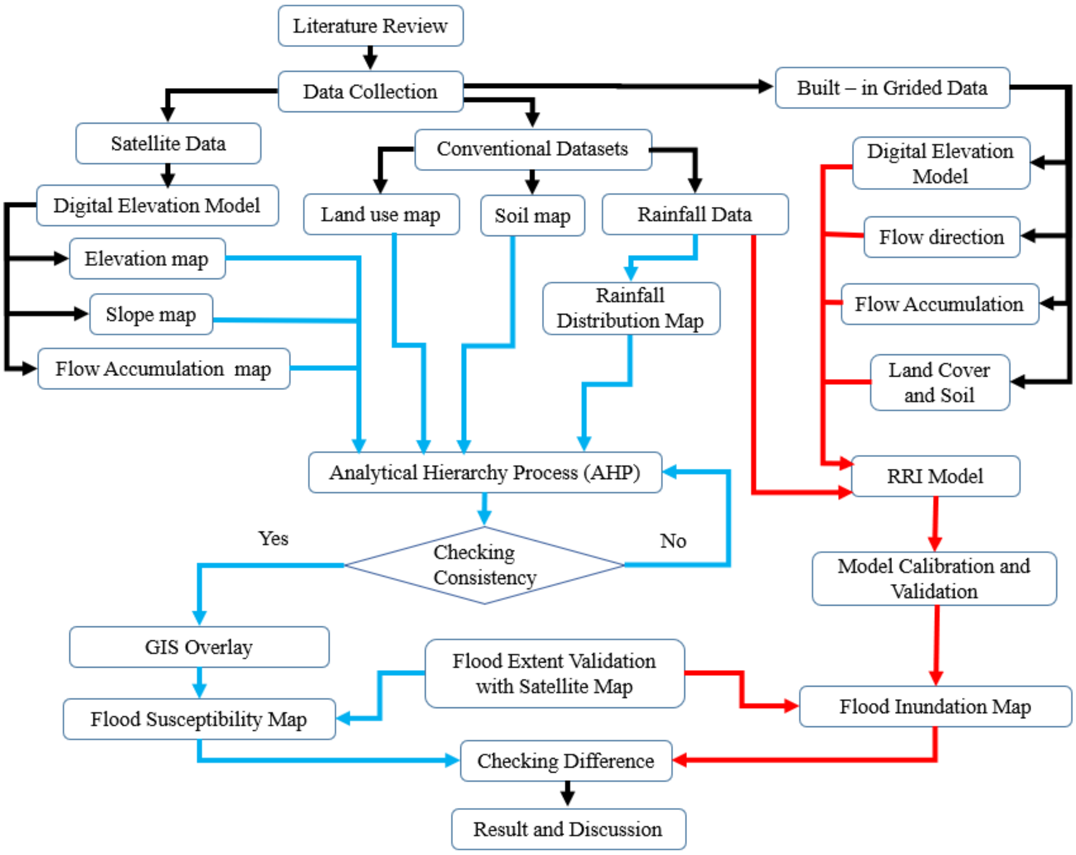


Figure 3-1: Methodology

## 3.1 Analytical Hierarchy Process (AHP)

The Analytical Hierarchy Process (AHP) includes the DEM data analysis, preprocessed maps, and the AHP procedure to obtain the flood susceptibility map.

### 3.1.1 DEM Data Analysis

The DEM resolutions of 12.5 m, 30 m, and 90 m were compared to select the best suitable DEM for the research. The 12.5 m DEM was obtained from ALOS PALSAR (https://earthdata.nasa.gov/) and the 30 m and 90 m DEM was obtained from SRTM (https://earthexplorer.usgs.gov/). The 12.5 m resolution DEM shows clear images for small areas. The 12.5 m resolution DEM is a very sensitive DEM resolution, and it shows a lot of patches in large areas. The 90 m resolution DEM is suitable for large areas, so the 90 m resolution DEM was used in this study as the study area (Kalu Ganga Basin) covers a very large area**.**

### 3.1.2 Pre-processed Maps

In the AHP process, satellite data (DEM) of 90 m resolution (from SRTM) was selected which is best suited for the study as the study area is large. The DEM was used to delineate Kalu Ganga Basin and prepare an elevation map and slope map. Flow accumulation was obtained by using the hydrology tool in ArcMap using the 90 m resolution DEM. Conventional data consisting of Land use and soil from the Survey Department was used to obtain a land-use map and soil map, respectively. The observed rainfall data were first checked for missing data and the missing data were filled. The rainfall data were used to obtain a rainfall distribution map using the IDW method in ArcMap. All the pre-processed maps are categorized into five classes (Das, 2018).

### 3.1.3 Analytical Hierarchy Process (AHP) Procedure

Once all the maps are pre-processed, the AHP model was applied to provide various weights to the parameters taken in this research. The AHP model was applied to obtain weights of parameters and ranks of subcategories for the flood susceptibility model.

The flood susceptibility index model is stated as follows (Saaty, 1980):

$$FS = \sum_{i=1}^{n} Wi\ x\ Ri \qquad [3\text{-}1]$$

where, FS is flood susceptibility index

Wi is weight of each parameter

Ri is the rank of rating of the classified values under a parameter.

The likelihood of flood occurrence was evaluated in this research by utilizing the FS model where the flood susceptibility map was arranged into four classes (Low, Moderate, High, and Very High). The AHP method in this paper contains two sections. The first section is the main arrangement of the parameters where all parameter values are given and weights are determined. The second section is built by ordering all the parameters into subcategories and obtaining their ranks. All the parameters considered in this review were studied individually and classified into different subcategories. Various positions were given to each subcategory through relative scoring utilizing the AHP strategy.

A pairwise examination framework was inherent in which the diagonal components were equivalent to 1. The overall significance of all the parameters was given dependent on various standards and qualities [(1) Equal Importance, (3) Moderate Importance, (5) Strong Importance, (7) Very Strong Importance, (9) Extreme Importance and (2, 4, 6, and 8) Intermediate Values) (Saaty, 1987). The scale of relative importance (Saaty, 1977) is given in Table 3-1.

Table 3-1: Scale of Relative Importance (Saaty, 1977)

| The intensity of Importance on an absolute scale | Definition | Explanation |
|---|---|---|
| 1 | Equal Importance | Two activities contribute equally to the objective |
| 3 | Moderate Importance | Experience and judgment strongly favor one activity over another |
| 5 | Strong Importance | Experience and judgment strongly favor one activity over another |
| 7 | Very Strong Importance | Activity is strongly favored, and its dominance demonstrated in practice |
| 9 | Extreme Importance | The evidence favoring one activity over another is of the highest possible order of affirmation |
| 2,4,6,8 | Intermediate Values | When compromise is needed |

In the pairwise examination matrix, the rows are the inverse value of each factor and its significance with others. The weighted arithmetic approach was utilized to ascertain the loads in the pairwise examination grid. The values in the pairwise matrix were normalized to obtain the normalized values. Afterward, the weights of the parameters were given by the mean row method in the pairwise examination matrix (Saaty, 1990).

The consistency was checked by the following equation (Saaty, 1980):

$$CR = \frac{CI}{RI} \quad [3\text{-}2]$$

$$CI = \frac{\lambda max\text{-}n}{n\text{-}1} \quad [3\text{-}3]$$

where, CR is consistency ratio

CI is consistency index

RI is random index

λmax is principal eigenvalue of matrix

n is number of components or factors in the matrix

The values of random inconsistency indices (RI) with respect to number of components (n) (Saaty, 1987) is shown in Table 3-2.

Table 3-2: Random Inconsistency Indices (Saaty, 1987)

| n | 3 | 4 | 5 | 6 | 7 | 8 | 9 | 10 |
|---|---|---|---|---|---|---|---|---|
| RI | 0.58 | 0.9 | 1.12 | 1.24 | 1.32 | 1.41 | 1.45 | 1.49 |

For this research, the consistency ratio (CR) is accepted if the value is less than 0.1, it demonstrates a good level for the pairwise correlation grid. In case of a consistency ratio (CR) greater than 0.1, the values of CR must be adjusted according to Saaty (1977).

After checking the consistency of the parameters and sub-classifications of parameters, the GIS overlay method was applied with the weighted sum function in ArcMap which includes the weights of the parameters and ranks of the sub-classifications as input data to obtain a flood susceptibility map. The final map was categorized into four classes (Low, Moderate, High, and Very High). The flood extent validation was carried out with the satellite maps.

### 3.2 Rainfall-Runoff-Inundation (RRI) Model

For RRI Model, the built-in grided data (digital elevation model (DEM), flow direction, flow accumulation, Land Cover and Soil) was used. The built-in grided data is in 30 Arc second resolution (900 m). Ground gauge rainfall data (event-based) was prepared as the input data (CSV format) and the RRI Model automatically convert it into Thiessen polygon. Along with Flood Inundation areas, the RRI model can also obtain flood depth and discharge. The model calibration and validation were done using the event-based method with the observed flood level. Two objective functions, NSC and $R^2$ were used for calibration and validation. The flood extents validation was carried out with the satellite maps (MODIS). Finally, the flood susceptibility map from the AHP method and flood inundation map from the RRI model was checked for their difference in the result section.

# CHAPTER 4

# 4 DATA CHECKING AND ANALYSIS

## 4.1 Data Collection

The detail of the data collection is shown in Table 4-1.

Table 4-1: Data Collection

| Data | Source | Data Type/Resolution |
|---|---|---|
| Precipitation | Meteorological Department, Sri Lanka | Daily (1970-2015) |
| Rainfall | Irrigation Department, Sri Lanka | Daily (1994-2013) |
| DEM | SRTM | 90 m |
| Soil Map | Survey Department, Sri Lanka | 1:50,000 (1998) |
| LULC Map | Survey Department, Sri Lanka | 1:50,000 (1999) |
| Satellite Flood Map (Priority Index Sri Lanka Floods May 2017) | HDX, OCHA | Sentinel-2 optical image and Sentinel-1 SAR image, 30 m Resolution (May 2017) |
| Affected DS Divisions by Floods and Landslides | PDNA Team | DMC and NBRO Data |
| Flood Level | Pre-Feasibility Study of Kalu Ganga Basin, Flood Management Model Report, Version No.3 | Event-based(masl) |
| Annual Maximum Flood Level of Kalu Ganga at Ratnapura | Irrigation Department of Sri Lanka | Annual Maximum Flood Level (masl) and Return Period |

The locations of rainfall and streamflow stations are shown in Table 4-2 and Table 4-3, respectively.

Table 4-2: Location of Rainfall Stations

| RF Stations | Co-ordinates (Degrees) | |
|---|---|---|
| | E | N |
| Alupolla | 80.58 | 6.72 |
| Lellopitiya | 80.50 | 6.68 |
| Ratnapura | 80.40 | 6.68 |
| Hapugasthenna | 80.52 | 6.72 |
| Galatura Estate | 80.28 | 6.70 |
| Halwatura | 80.20 | 6.72 |
| Rayigama | 80.18 | 6.77 |
| Sirikandura | 80.15 | 6.50 |
| Horana | 80.07 | 6.75 |
| Clyde Estate | 80.03 | 6.58 |
| Kalutara | 79.95 | 6.58 |

Table 4-3: Location of Streamflow Stations

| SF Station | Co-ordinates (Degrees) | |
|---|---|---|
| | E | N |
| Ellagawa | 80.21 | 6.73 |
| Millakanda | 80.16 | 6.63 |
| Putupaula | 80.06 | 6.61 |

The map with the locations of the rainfall and streamflow stations is shown in Figure 4-1.

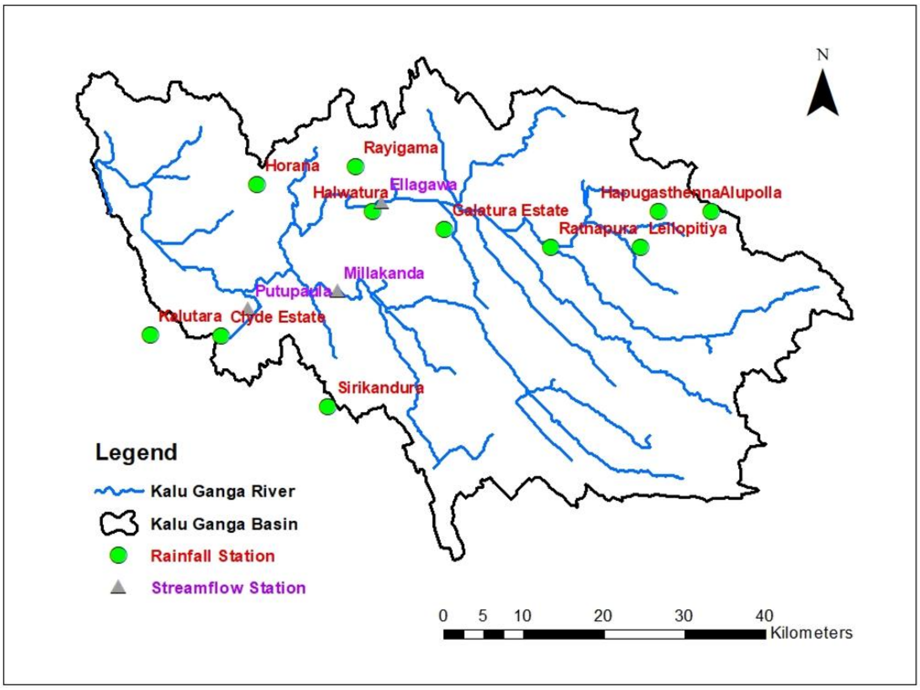


Figure 4-1: Locations of Rainfall and Streamflow Stations

## 4.2 Rainfall Data Checking

Rainfall data were collected for eleven rainfall stations (1970-2015). Visual data checking was carried out to check the missing data. There were no missing data from 1970 to 2009. After 2009, the missing rainfall data information is shown in Table 4-4.

Table 4-4: Missing Rainfall Data

| RF Stations | Missing Data (%) |
|---|---|
| Alupolla | 0.37 |
| Lellopitiya | 3.24 |
| Ratnapura | 0.00 |
| Hapugasthenna | 0.18 |
| Galatura Estate | 1.45 |
| Halwatura | 0.36 |
| Rayigama | 0.91 |
| Sirikandura | 0.36 |
| Horana | 1.07 |
| Clyde Estate | 0.36 |
| Kalutara | 0.92 |

## 4.3 Filling Missing Rainfall Data

Missing data were analyzed by using the methods stated by Subramany (2019). If the annual average rainfall difference between the two stations is less than 10%, then a simple arithmetic average procedure is followed to estimate the missing rainfall values. If the difference is greater than 10%, the normal ratio method is used (Subramanya, 2013).

Sample Calculation:

Annual Average Rainfall at Halwatura Station = 4,141 mm

Annual Average Rainfall at Galatura Estate Station = 4,029 mm

Annual Average Rainfall at Rayigama Station = 3,778 mm

The difference in Annual Average Rainfall between Halwatura Station and Galatura Estate Station = ((4,141-4,029)/4,141) *100

= 2.7%

Difference in Annual Average Rainfall between Halwatura Station and Rayigama Station = ((4,141-3,778)/4,141) *100

= 8.7%

The difference was less than 10% therefore, the missing rainfall data were filled with the simple arithmetic average procedure.

The single mass curve (annual) of all the stations was plotted in one graph and the double mass curve (daily) of all the stations was plotted to check the consistency of rainfall data after filling all the missing rainfall data. The single mass curve after filling all the missing rainfall data is shown in Figure 4-2.

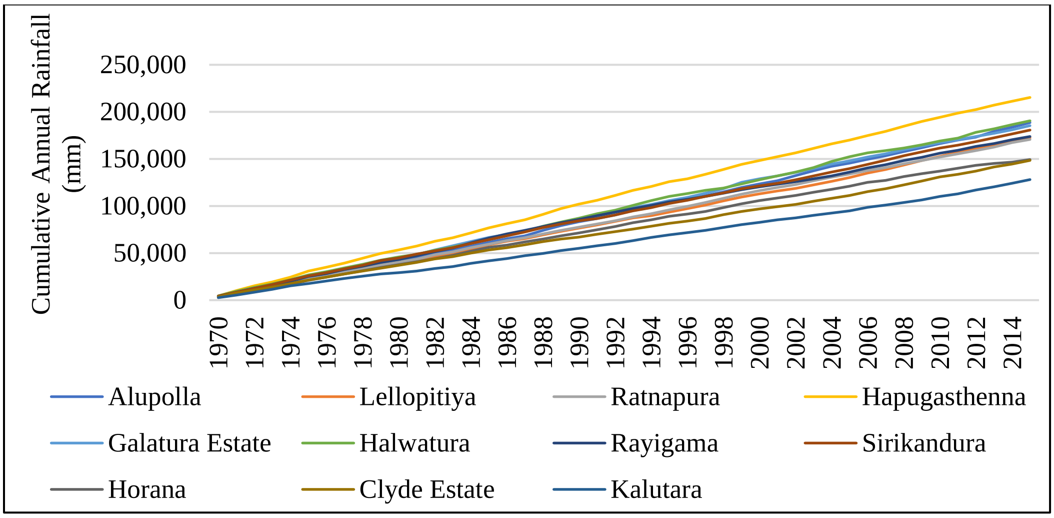


Figure 4-2: Single Mass Curve of Annual Rainfall (All Stations)

The single mass curve of all the stations shows Hapugasthenna station with high cumulative annual rainfall indicating Hapugasthenna station receiving high rainfalls and Rayigama station with low cumulative annual rainfall indicating Rayigama station receiving low rainfalls. Other station shows a similar pattern of cumulative annual rainfall between the stations indicating the stations receiving a similar pattern of rainfall.

The double mass curve (daily) of the Halwatura station after filling all the missing rainfall data is shown in Figure 4-3. The double mass curve of all the stations after filling the missing rainfall data is shown in annexure 1.

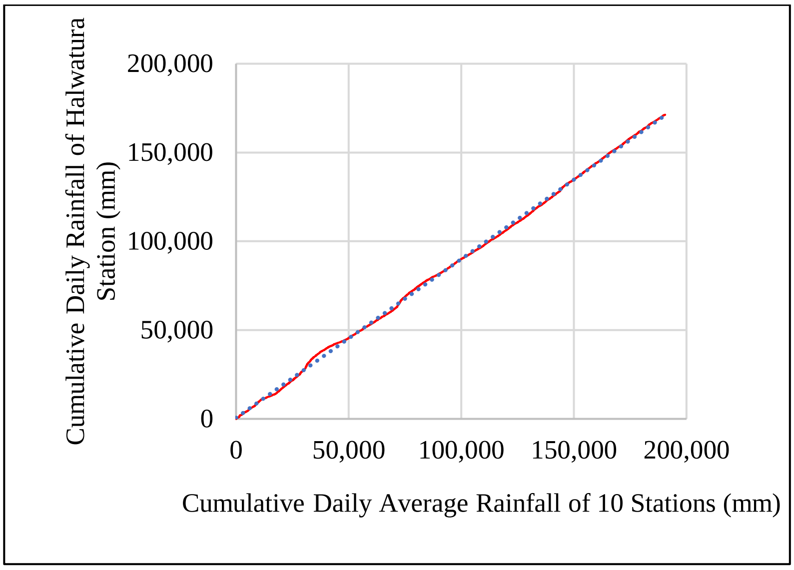


Figure 4-3: Double Mass Curve – Halwatura

The double mass curve of Halwatura station after filling all the missing rainfall data shows a good match between cumulative daily rainfall of Halwatura Station and a cumulative daily average rainfall of ten (10) Stations.

## 4.4 Streamflow Data Checking

Streamflow data were collected for Ellagawa, Millakanda and Putupaula streamflow stations (1994 - 2013). Visual data checking was carried out to check the missing data. The missing streamflow data information is shown in Table 4-5.

Table 4-5: Missing Streamflow Data

| SF Station | Missing Data (%) |
|---|---|
| Ellagawa | 1.25 |
| Millakanda | 1.30 |
| Putupaula | 1.18 |

The missing streamflow data were filled with a simple arithmetic average procedure. The daily streamflow versus daily rainfall graph was plotted to check the rainfall and streamflow data after filling all the missing data. Ellagawa streamflow station was taken as the reference streamflow station with other rainfall stations while plotting the daily streamflow versus daily rainfall graphs. The daily streamflow versus daily rainfall graph of Ellagawa SF station and Halwatura RF station after filling all the missing data is shown in Figure 4-4. The daily streamflow versus daily rainfall graph of all the stations after filling the missing data is shown in annexure 2.

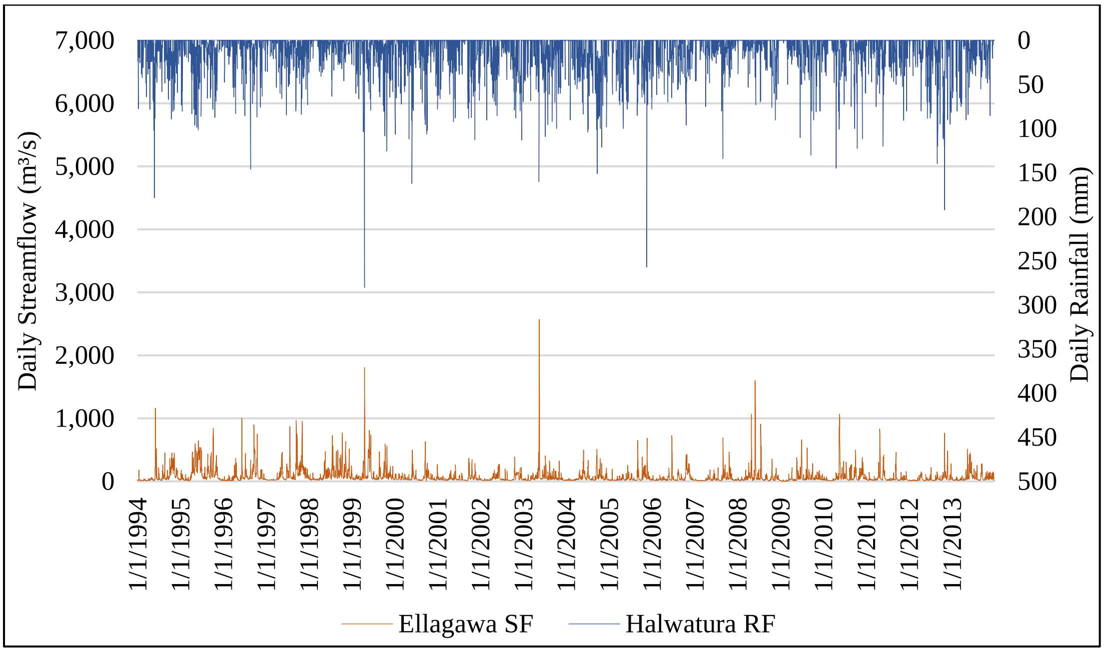


Figure 4-4: Ellagawa Streamflow Versus Halwatura Rainfall

The daily streamflow versus daily rainfall graph of Ellagawa SF station and Halwatura RF station after filling the missing data shows a matching pattern between the Ellagawa SF and Halwatura RF.

# CHAPTER 5

# 5 MODEL DEVELOPMENT AND APPLICATIONS

## 5.1 Analytical Hierarchy Process (AHP)

The Analytical Hierarchy Process (AHP) method includes preparation of preprocessed maps, obtaining weights of the parameters and ranks of the subcategories, and finally overlaying the preprocessed maps with the weights and ranks using the weighted sum function in ArcMap to obtain the flood susceptibility map.

### 5.1.1 Pre-processed Maps

The preprocessed maps of all the six parameters are shown in Figure 5-1 (Elevation map), Figure 5-2 (Slope map), Figure 5-3 (Slope map), Figure 5-4 (Soil map), Figure 5-5 (Land-use map) and Figure 5-6 (Rainfall Distribution map).

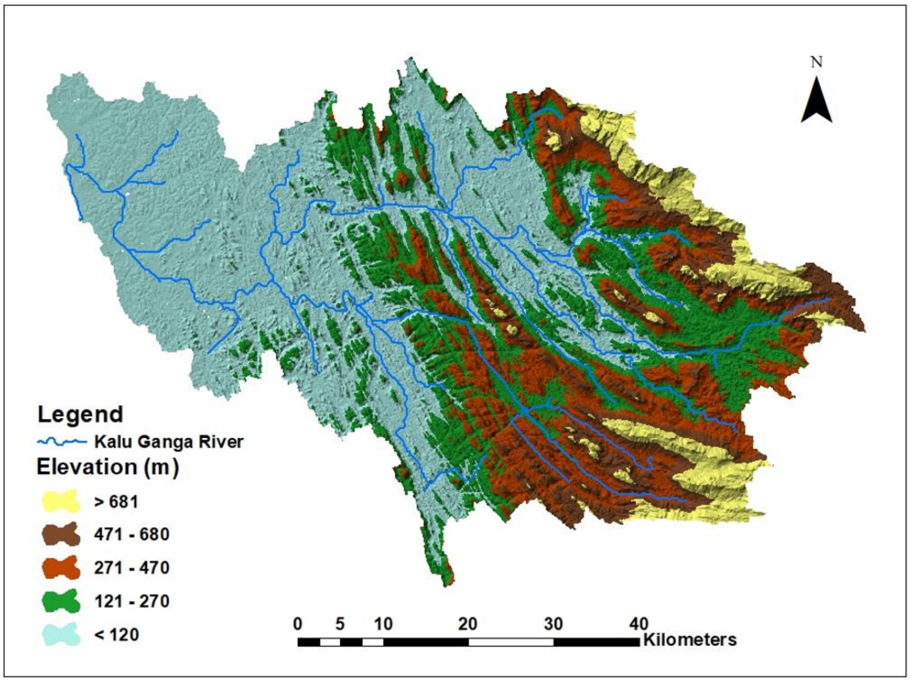


Figure 5-1: Elevation Map

(*Source: SRTM, Resolution 90 m*)

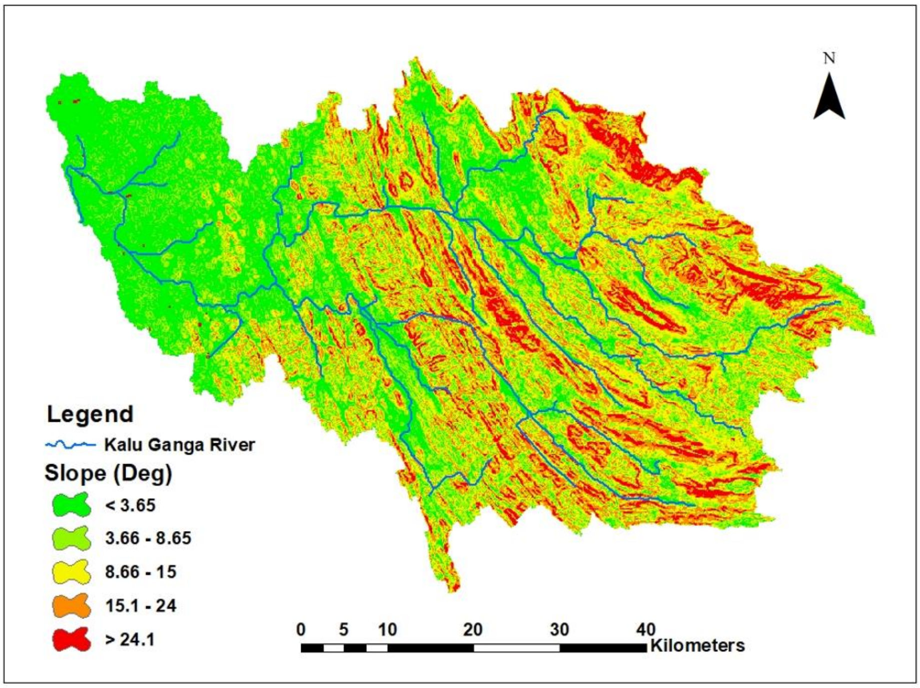


Figure 5-2: Slope Map

(*Source: SRTM, Resolution 90 m*)

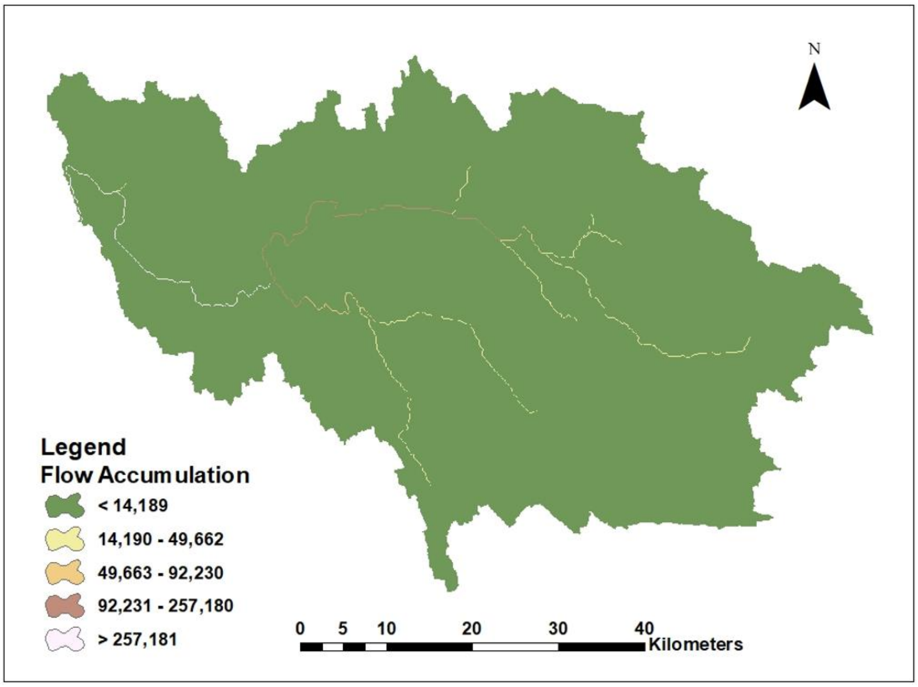


Figure 5-3: Flow Accumulation Map

(*Source: SRTM, Resolution 90 m*)

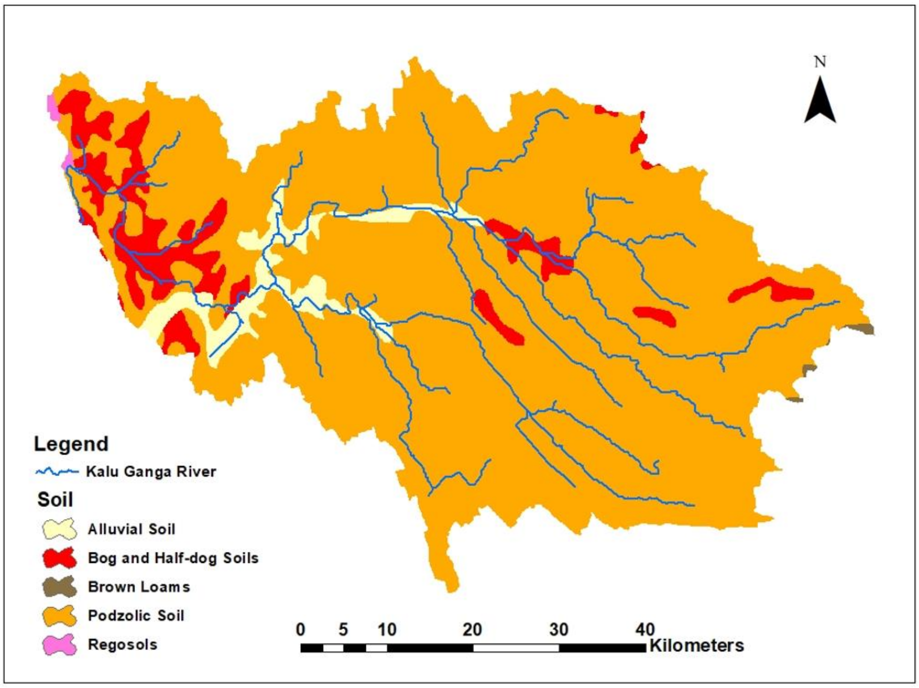


Figure 5-4: Soil Map

(*Source: Survey Department of Sri Lanka, 1998*)

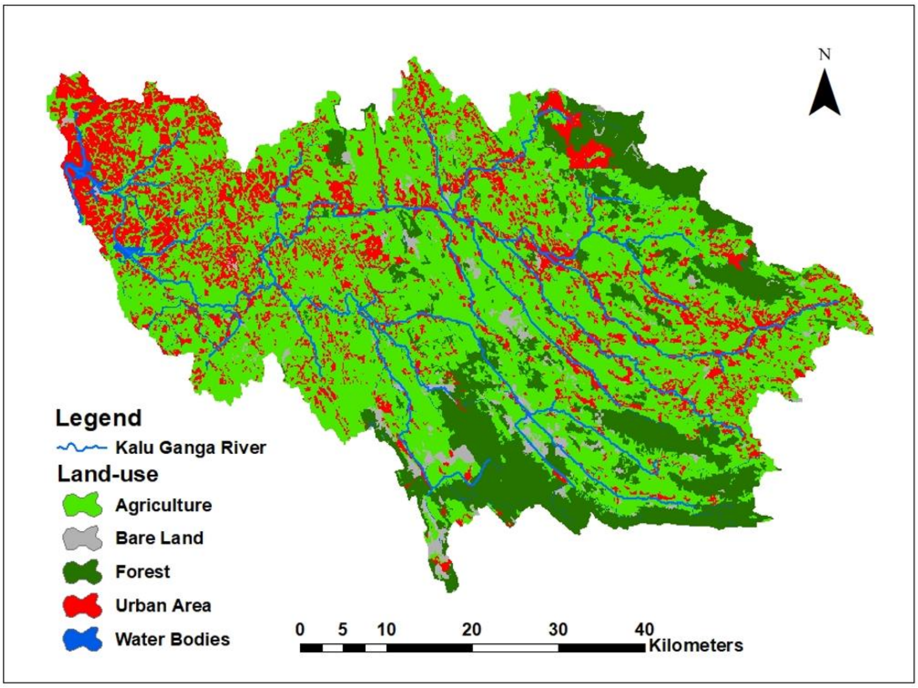


Figure 5-5: Land-use Map

(*Source: Survey Department of Sri Lanka, 1999*)

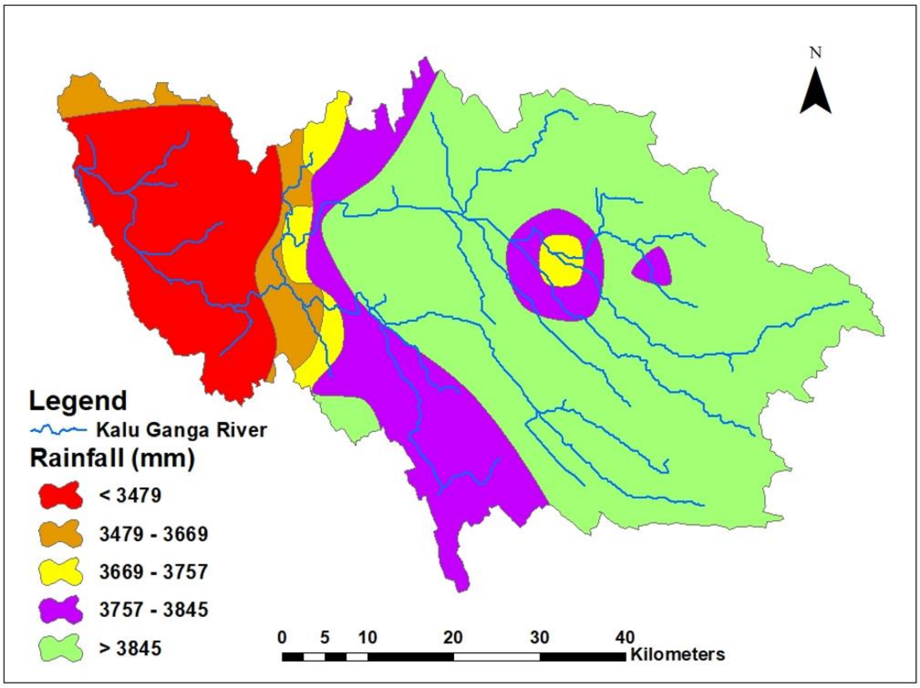


Figure 5-6: Rainfall Distribution Map

### 5.1.2 Analytical Hierarchy Process (AHP) Procedure

The pairwise comparison framework and value of each parameter are shown in Table 5-1. The normalized framework and weight value in the pairwise comparison framework are shown in Table 5-2. The weighted flood susceptibility index is shown in Table 5-3. The pairwise comparison matrix and score of subcategories are shown in annexure 3.

Table 5-1: Pairwise Comparison Matrix and Score of Each Parameter

| Parameter | Elevation | Slope | Flow Accumulation | Soil | Land-use | Rainfall |
|---|---|---|---|---|---|---|
| Elevation | 1 | 2 | 4 | 7 | 5 | 3 |
| Slope | 1/2 | 1 | 3 | 5 | 5 | 2 |
| Flow Accumulation | 1/4 | 1/3 | 1 | 3 | 2 | 1/2 |
| Soil | 1/7 | 1/5 | 1/3 | 1 | 1/2 | 1/4 |
| Land-use | 1/5 | 1/5 | 1/2 | 2 | 1 | 1/3 |
| Rainfall | 1/3 | 1/2 | 2 | 4 | 3 | 1 |

Table 5-2: Normalized and Weight Values in Pairwise Comparison Matrix

| Parameter | Elevation | Slope | Flow Accumulation | Soil | Land-use | Rainfall | Weight | Rank | CR |
|---|---|---|---|---|---|---|---|---|---|
| Elevation | 0.41 | 0.47 | 0.37 | 0.32 | 0.3 | 0.42 | 0.38 | 1 | 0.018 |
| Slope | 0.21 | 0.24 | 0.28 | 0.23 | 0.3 | 0.28 | 0.26 | 2 | |
| Flow Accumulation | 0.1 | 0.08 | 0.09 | 0.14 | 0.12 | 0.07 | 0.1 | 4 | |
| Soil | 0.06 | 0.05 | 0.03 | 0.05 | 0.03 | 0.04 | 0.04 | 6 | |
| Land-use | 0.08 | 0.05 | 0.05 | 0.09 | 0.06 | 0.05 | 0.06 | 5 | |
| Rainfall | 0.14 | 0.12 | 0.18 | 0.18 | 0.18 | 0.14 | 0.16 | 3 | |

Table 5-3: Weighted Flood Susceptibility Index

| Parameter | Subcategories | Weight (Wi) | Rank (Ri) | Overall Weightage (FS=Wi x Ri) |
|---|---|---|---|---|
| Elevation (mm) | > 681 | 38 | 1 | 38 |
| | 471 - 680 | | 2 | 76 |
| | 271 - 470 | | 3 | 114 |
| | 121 - 270 | | 4 | 152 |
| | < 120 | | 5 | 190 |
| Slope (Degree) | > 24.1 | 26 | 1 | 26 |
| | 15.1 - 24 | | 2 | 52 |
| | 8.65 - 15 | | 3 | 78 |
| | 3.66 - 8.65 | | 4 | 104 |
| | < 3.65 | | 5 | 130 |
| Flow Accumulation | < 14,189 | 10 | 1 | 10 |
| | 14,190 - 49,662 | | 2 | 20 |
| | 19,663 - 92,230 | | 3 | 30 |
| | 92,231- 257,180 | | 4 | 40 |
| | > 257,181 | | 5 | 50 |
| Soil | Brown Loams | 4 | 1 | 4 |
| | Regosols | | 2 | 8 |
| | Podzolic Soils | | 3 | 12 |
| | Bog and Half-dog Soil | | 4 | 16 |
| | Alluvial Soil | | 5 | 20 |
| Rainfall (mm) | < 3479 | 16 | 1 | 16 |
| | 3479 - 3669 | | 2 | 32 |
| | 3669 - 3757 | | 3 | 48 |
| | 3757 - 3845 | | 4 | 64 |
| | > 3845 | | 5 | 80 |

## 5.2 Rainfall-Runoff-Inundation (RRI) Model

There were major flood events in Kalu Ganga Basin from 16th to 18th of May 2003 and from 27th to 29th of April 2008. Rainfall data from 16th to 23rd of May 2003 was used in the RRI Model for model calibration and from 27th April to 5th of May 2008 and from 30th May to 7th of June 2008 for model validation. The RRI model calibration and validation were done by adjusting the *nr* river value and *ns* slope value (Onjira & Sayama, 2014). The model was calibrated and validated with the observed flood level. Objective functions, NSC and $R^2$ were used for calibration and validation. The events were taken considering the return period (Irrigation Department of Sri Lanka). The events of 5th September 2005, 29th April 2011, and 19th May 2013 were used to validate the RRI model flood inundation extent with MODIS satellite image.

### 5.2.1 RRI Model Calibration (May 2003)

The model calibration of May 2003 was obtained with an *nr* river value of 0.03 $m^{-1/3}s$ and an *ns* slope value of 0.4 $m^{-1/3}s$. The model calibration of May 2003 was carried out with flood levels at four sites (Ratnapura, Ellagawa, Millakanda, and Putupaula) during the flood period. Figure 5-7 to 5-10 shows the calibration results of May 2003.

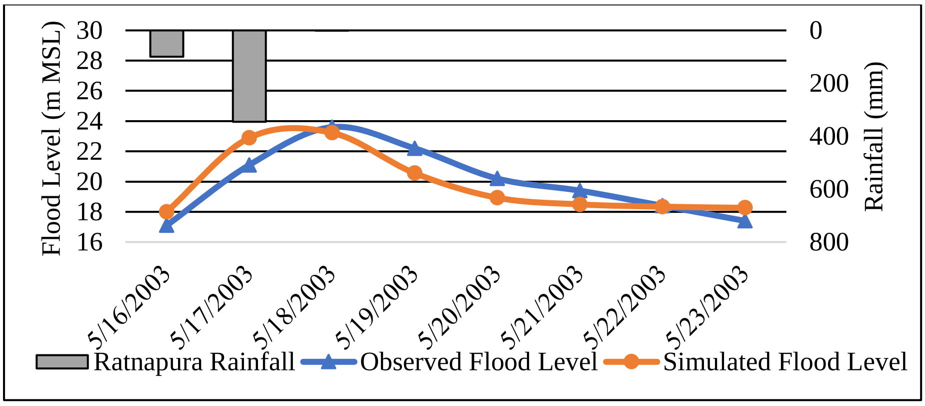


Figure 5-7: RRI Model Calibration of May 2003 at Ratnapura

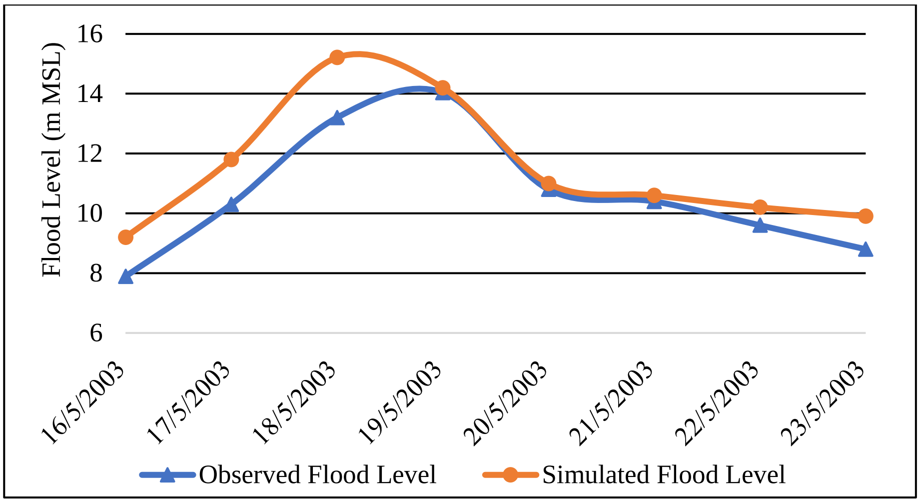


Figure 5-8: RRI Model Calibration of May 2003 at Ellagawa

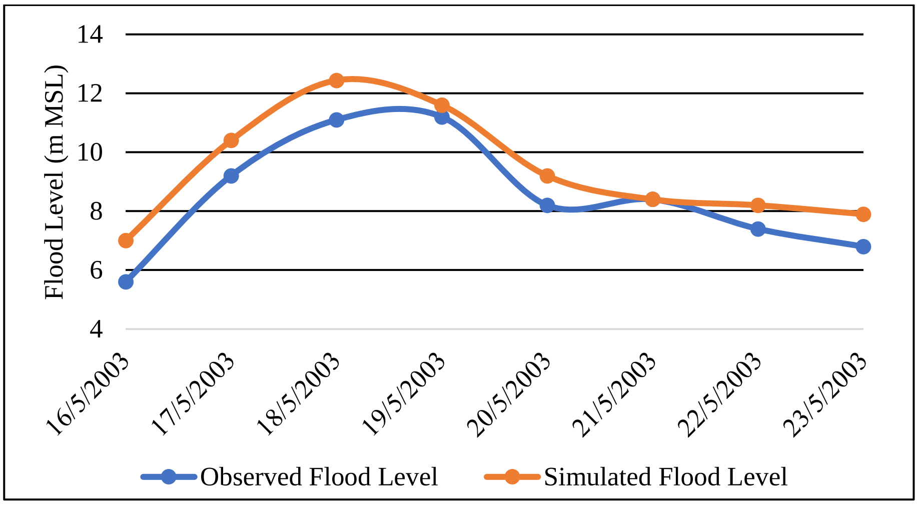


Figure 5-9: RRI Model Calibration of May 2003 at Millakanda

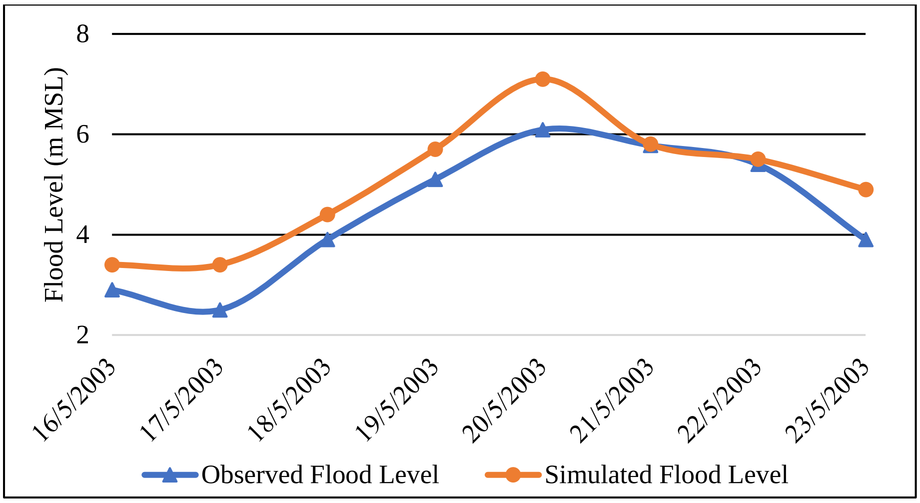


Figure 5-10: RRI Model Calibration of May 2003 at Putupaula

Table 5-4: RRI Model Calibration - May 2003

| Station | NSE | Remark | $R^2$ | Remark |
|---|---|---|---|---|
| Ratnapura | 0.73 | Good | 0.75 | Good |
| Ellagawa | 0.68 | Satisfactory | 0.89 | Very Good |
| Millakanda | 0.70 | Good | 0.93 | Very Good |
| Putupaula | 0.71 | Good | 0.91 | Very Good |

Table 5-4 shows the model calibration result of May 2003. Calibration results of May 2003 show Good NSE result in Ratnapura, Millakanda, and Putupaula sites whereas, in Ellagawa, it was satisfactory. Calibration results of May 2003 show Very Good $R^2$ result in Ellagawa, Millakanda, and Putupaula sites whereas, in Ratnapura, it was Good. The event of May 2003 has a return period of 31 years.

### 5.2.2 RRI Model Validation (April 2008)

The model validation of April 2008 was obtained with an *nr* river value of 0.03 $m^{-1/3}s$ and an *ns* slope value of 0.4 $m^{-1/3}s$. The model validation of April 2008 was carried out with flood levels at four sites (Ratnapura, Ellagawa, Millakanda, and Putupaula) during the flood period. Figure 5-11 to 5-14 shows the validation results of April 2008.

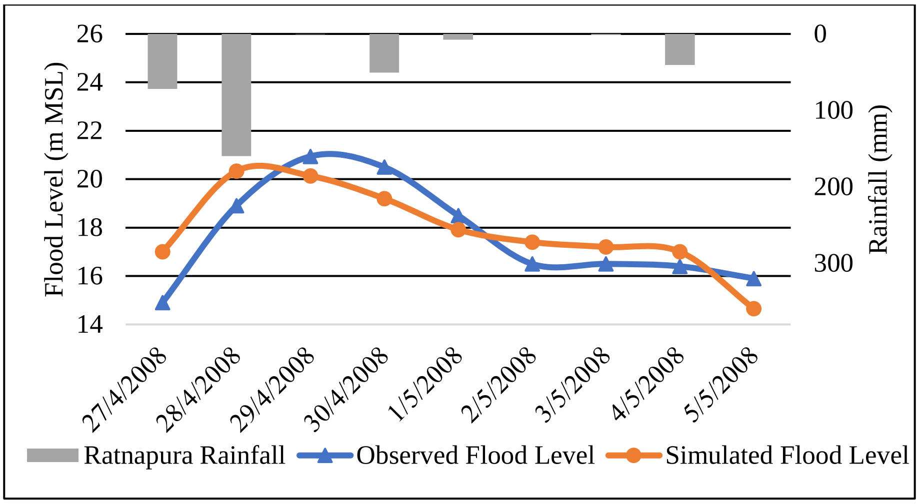


Figure 5-11: RRI Model Validation of April 2008 at Ratnapura

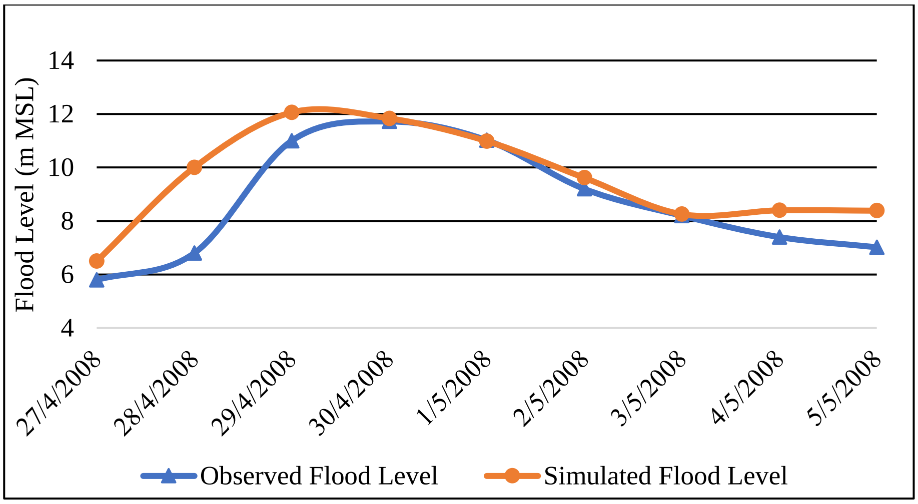


Figure 5-12: RRI Model Validation of April 2008 at Ellagawa

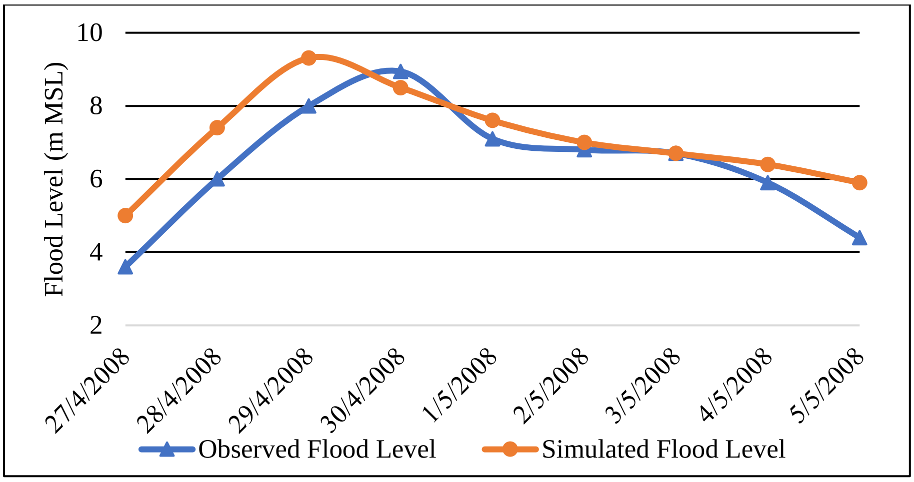


Figure 5-13: RRI Model Validation of April 2008 at Millakanda

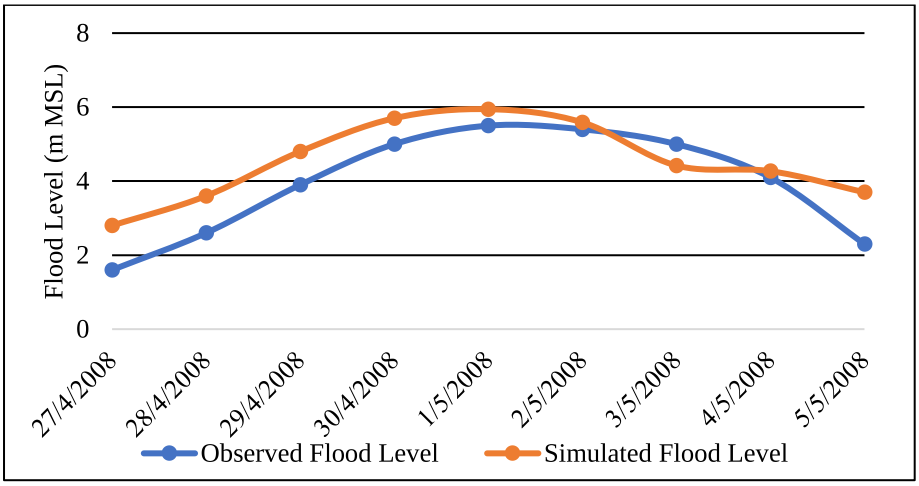


Figure 5-14: RRI Model Validation of April 2008 at Putupaula

Table 5-5: RRI Model Validation - April 2008

| Station | NSE | Remark | $R^2$ | Remark |
|---|---|---|---|---|
| Ratnapura | 0.65 | Satisfactory | 0.67 | Satisfactory |
| Ellagawa | 0.59 | Satisfactory | 0.78 | Good |
| Millakanda | 0.61 | Satisfactory | 0.83 | Good |
| Putupaula | 0.62 | Satisfactory | 0.85 | Good |

Table 5-5 shows the model validation result of April 2008. Validation results of April 2008 show Satisfactory NSE result in Ratnapura, Ellagawa, Millakanda, and Putupaula sites. Validation results of April 2008 show Good $R^2$ result in Ellagawa, Millakanda, and Putupaula sites whereas, in Ratnapura, it was Satisfactory. The event of April 2008 has a return period of 8 years.

### 5.2.3 RRI Model Validation (May 2008)

The model validation of May 2008 was obtained with an *nr* river value of 0.03 $m^{-1/3}s$ and an *ns* slope value of 0.4 $m^{-1/3}s$. The model validation of May 2008 was carried out with flood levels at four sites (Ratnapura, Ellagawa, Millakanda, and Putupaula) during the flood period. Figure 5-15 to 5-18 shows the validation results of May 2008.

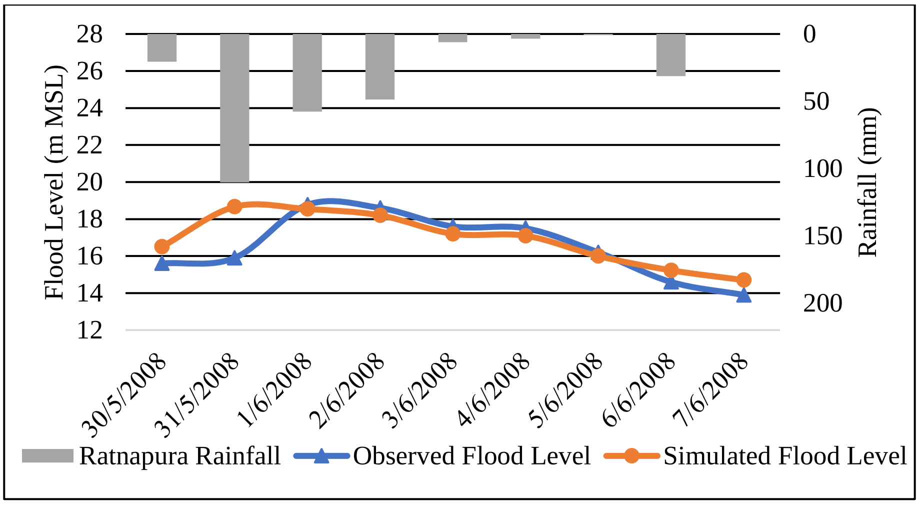


Figure 5-15: RRI Model Validation of May 2008 at Ratnapura

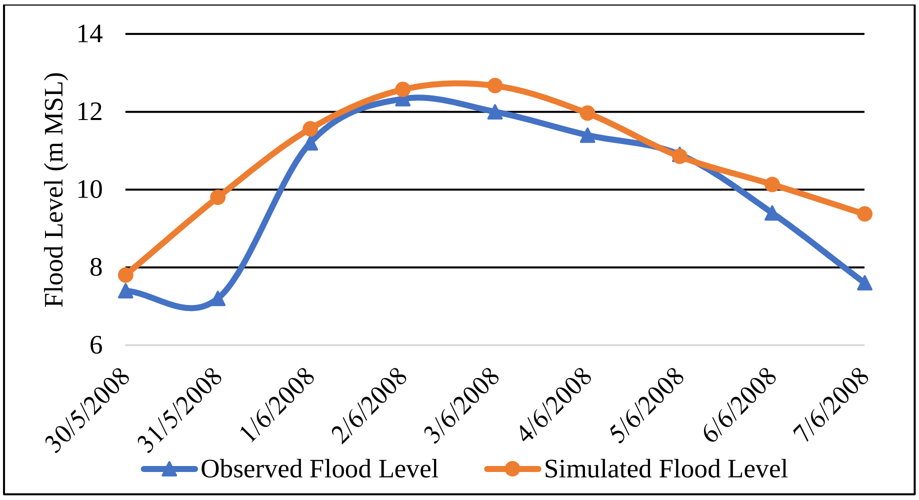


Figure 5-16: RRI Model Validation of May 2008 at Ellagawa

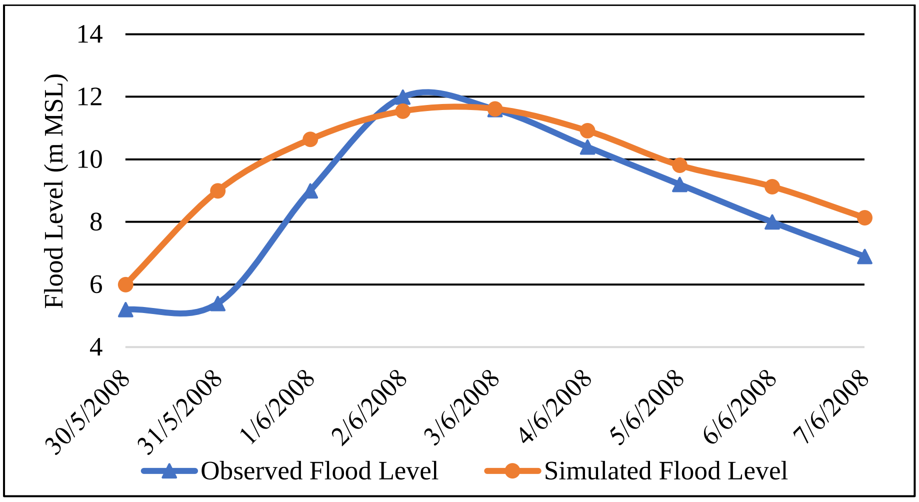


Figure 5-17: RRI Model Validation of May 2008 at Millakanda

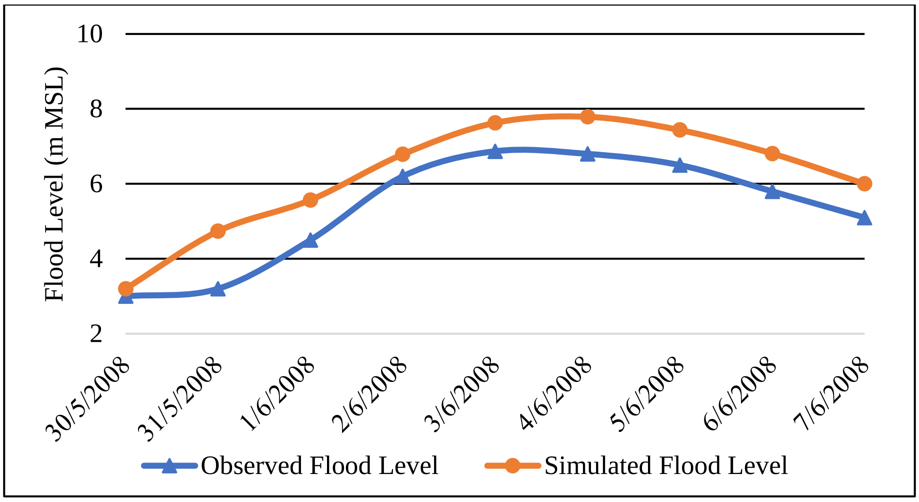


Figure 5-18: RRI Model Validation of May 2008 at Putupaula

Table 5-6: RRI Model Validation - May 2008

| Station | NSE | Remark | $R^2$ | Remark |
|---|---|---|---|---|
| Ratnapura | 0.57 | Satisfactory | 0.63 | Satisfactory |
| Ellagawa | 0.66 | Satisfactory | 0.85 | Good |
| Millakanda | 0.59 | Satisfactory | 0.81 | Good |
| Putupaula | 0.54 | Satisfactory | 0.94 | Very Good |

Table 5-6 shows the model validation result of May 2008. Validation results of May 2008 show Satisfactory NSE result in Ratnapura, Ellagawa, Millakanda, and Putupaula sites. Validation results of May 2008 show Very Good $R^2$ result in Putupaula, Good in Ellagawa and Millakanda sites and Satisfactory in Ratnapura. The event of May 2008 has a return period of 8 years.

# CHAPTER 6

## 6 RESULTS AND ANALYSIS

### 6.1 Analytical Hierarchy Process (AHP)

A flood susceptibility map of the Kalu Ganga basin was obtained using the AHP method.

#### 6.1.1 Flood Susceptibility Map using AHP Method

The flood susceptibility map of the Kalu Ganga basin is shown in Figure 6-1.

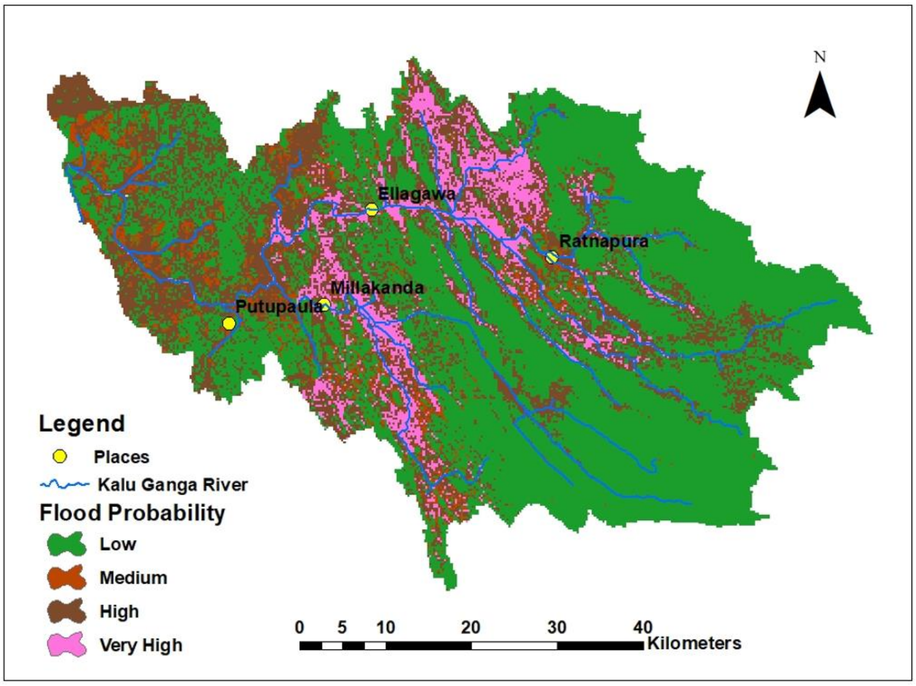


Figure 6-1: Flood Susceptibility Map

Using the AHP method in ArcMap, a flood probability map was obtained. The flood probability map shows the likelihood of the flood occurrence in Kalu Ganga Basin. The flood probability of the Very High and High category can be considered as the area with the most likelihood of flood occurrence in the Kalu Ganga Basin. The lower basin area has a high category flood probability area mainly influenced by the rainfall parameter whereby the lower area experienced lower rainfall as per the observed rainfall data. Ellagawa and Millakanda areas have Very High category flood probability areas whereas Ratnapura and Putupaula areas have High category flood probability areas.

### 6.1.2 Flood Extent Validation for Flood Susceptibility Map

The flood extents of flood susceptibility map were validated with Priority Index Sri Lanka Floods May 2017 map and affected DS Divisions by floods and landslides May 2017 map.

**Priority Index Sri Lanka Floods May 2017.**

The Priority Index Sri Lanka Floods May 2017 map is shown in Figure 6-2.

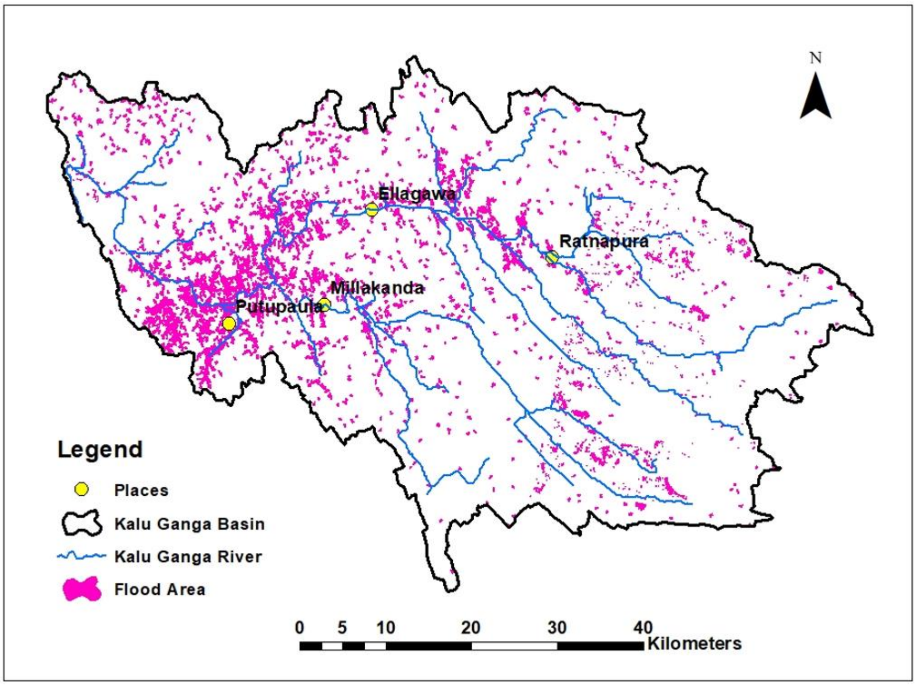


Figure 6-2: Priority Index Sri Lanka Floods Map - May 2017

(*Source: HDX*, *OCHA*)

The Priority Index Sri Lanka Floods May 2017 was analyzed using Sentinel-2 optical image (28th May 2017) and Sentinel-1 SAR image (30th May 2017). The resolution of the flood extent map is 30 m. The flood map is obtained from Humanitarian Data

Exchange (HDX), United Nations Office for the Coordination of Humanitarian Affairs (OCHA)(https://data.humdata.org/dataset/priority-index-sri-lanka-floods-may-2017). The flood map shows high flood areas in the Putupaula area and fewer flood areas in Ratnapura, Ellagawa, and Millakanda areas. The flood susceptibility map matches with the Priority Index Sri Lanka Floods May 2017 map in the lower basin.

**Affected DS Divisions by Floods and Landslides May 2017**

The affected DS Divisions by floods and landslides May 2017 map is shown in Figure 6-3.

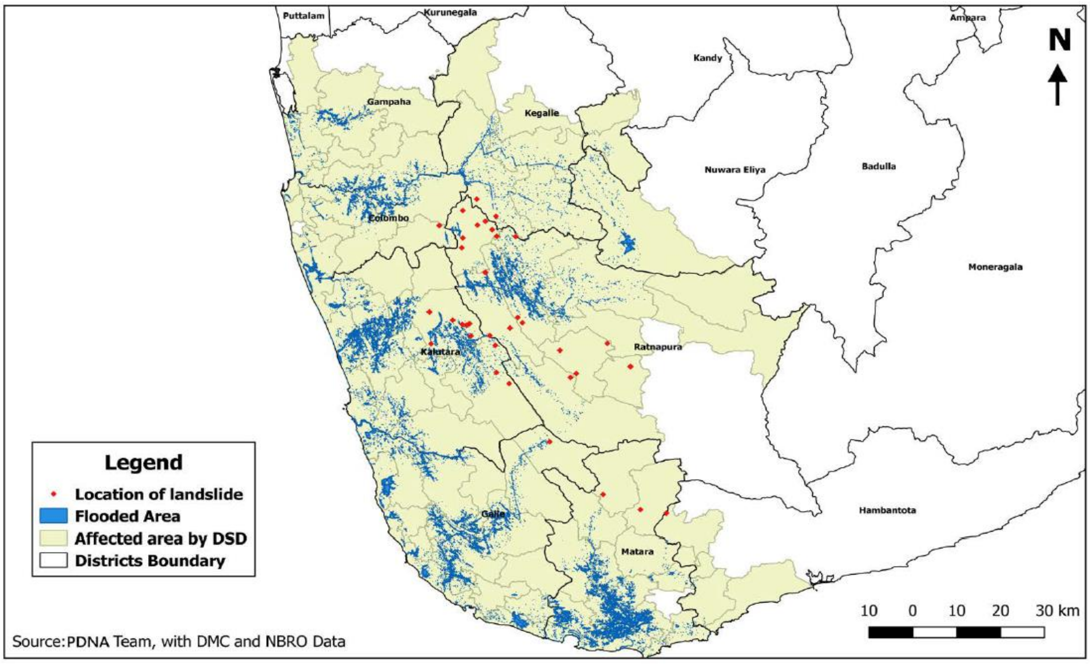


Figure 6-3: Affected DS Divisions by Floods and Landslides Map - May 2017

(*Source: PDNA, 2017*)

The Post Disaster Needs Assessment (PDNA) – Sri Lanka May 2017 shows the affected DS Divisions by floods and landslides. The PDNA – Sri Lanka May 2017 is obtained from PDNA (2017) with Disaster Management Centre (DMC) and National Building Research Organization (NBRO) Data. The PDNA –Sri Lanka May 2017 is prepared by PDNA Team. The PDNA – Sri Lanka May 2017 shows high flood areas in Ratnapura, Ellagawa, Millakanda and Putupaula areas. The flood susceptibility map matches with the affected DS divisions by floods and landslides May 2017 map in Ratnapura, Ellagawa, Millakanda, and Putupaula areas.

## 6.2 Rainfall-Runoff-Inundation (RRI) Model

The calibration and validation results of the RRI model showed acceptable agreement between simulated results and observed data indicating that the RRI model with built-in data can simulate efficiently the inundation area in the Kalu Ganga basin.

Flood inundation maps of May 2003, April 2008, and May 2008 were obtained using the RRI model.

### 6.2.1 Flood Inundation Maps

Figure 6-4 to Figure 6-6 shows the flood inundation maps of May 2003, April 2008, and May 2008, respectively, obtained from the RRI Model.

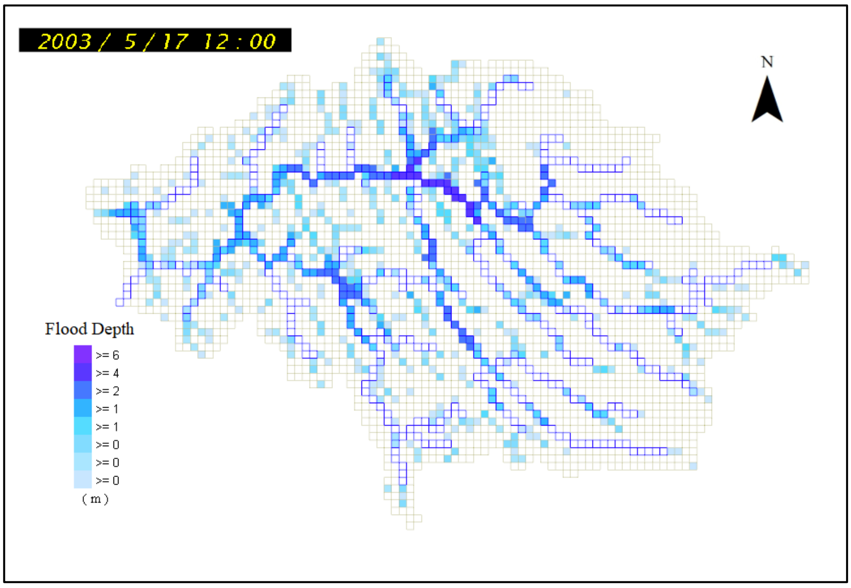


Figure 6-4: Flood Inundation Map – 17th May 2003

The flood inundation map of May 2003 shows the Ratnapura area with flood depths greater than or equivalent to 4 meters. Ellagawa, Millakanda, and Putupaula areas have flood depths greater than or equivalent to 2 meters.

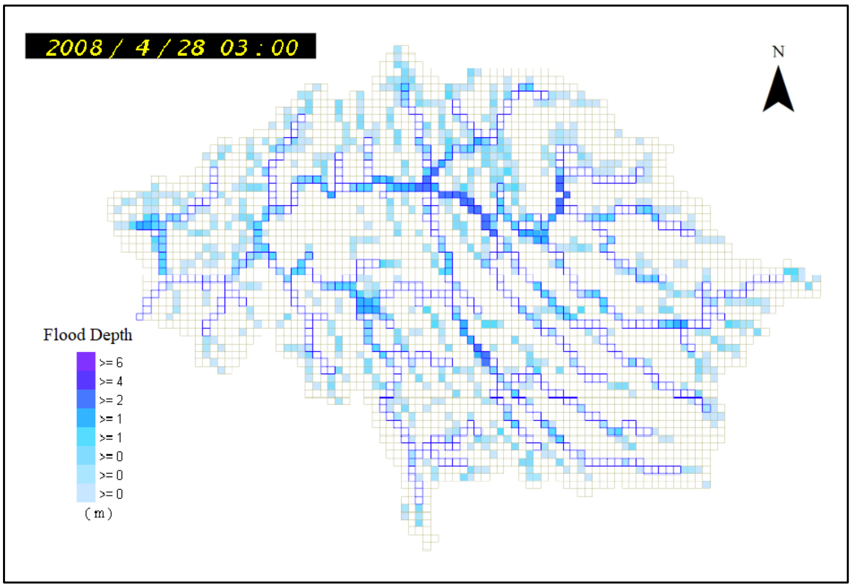


Figure 6-5: Flood Inundation Map – 28th April 2008

The flood inundation map of April 2008 shows the Ratnapura area with flood depths greater than or equivalent to 2 meters. Ellagawa, Millakanda, and Putupaula areas have flood depths greater than or equivalent to 1 meter.

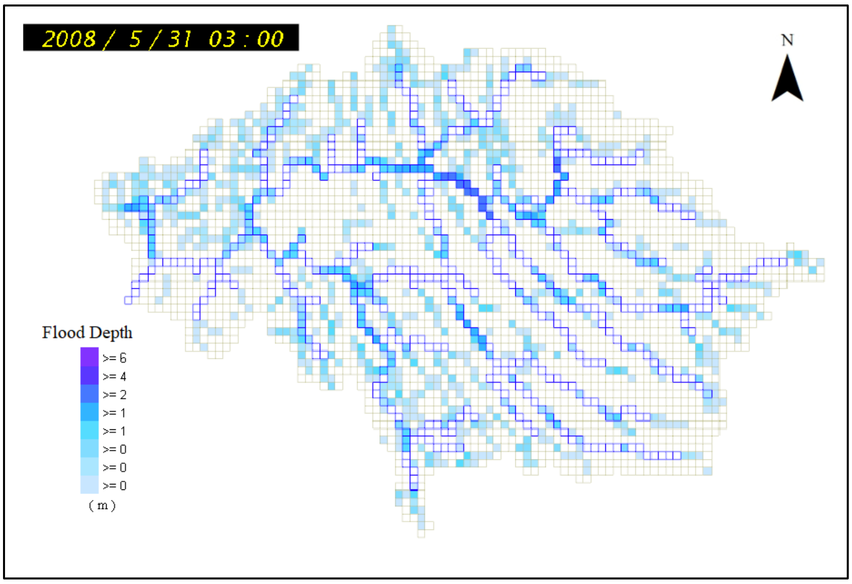


Figure 6-6: Flood Inundation Map – 31st May 2008

The flood inundation map of May 2008 shows the Ratnapura area with flood depths greater than or equivalent to 2 meters. Ellagawa, Millakanda, and Putupaula areas have flood depths greater than or equivalent to 1 meter.

### 6.2.2 Flood Extent Validation for Flood Inundation Map

The MODIS image of May 2003 (Calibration) had the whole basin covered with cloud cover and the MODIS data was not available for April and May 2008 (Validation). So, the MODIS image of those events couldn't be used for flood extent validation. MODIS image is downloaded for three events 5th September 2005, 29th April 2011, and 19th May 2013 for flood extent validation. The MODIS image was used to validate the event-based RRI model flood inundation extent.

**Flood Map - 5th September 2005**

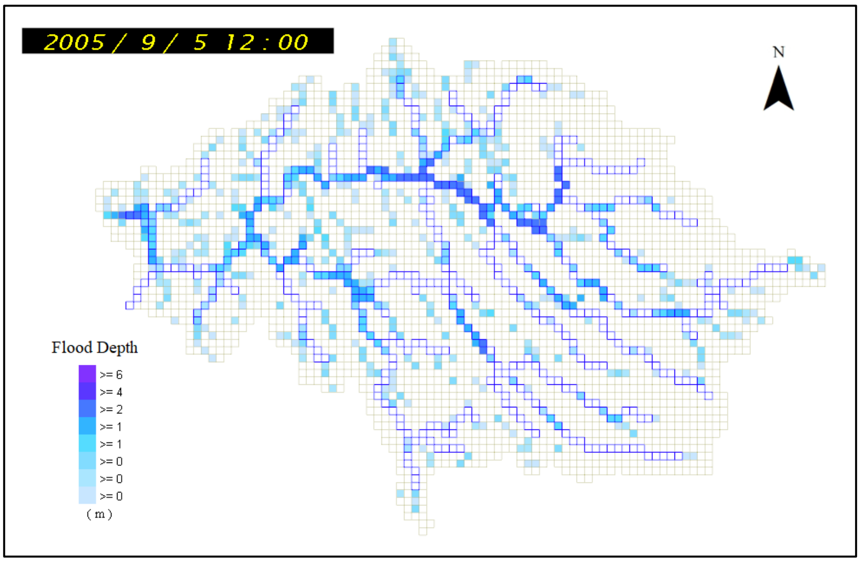


Figure 6-7: Flood Inundation Map – 5th September 2005 (RRI Model)

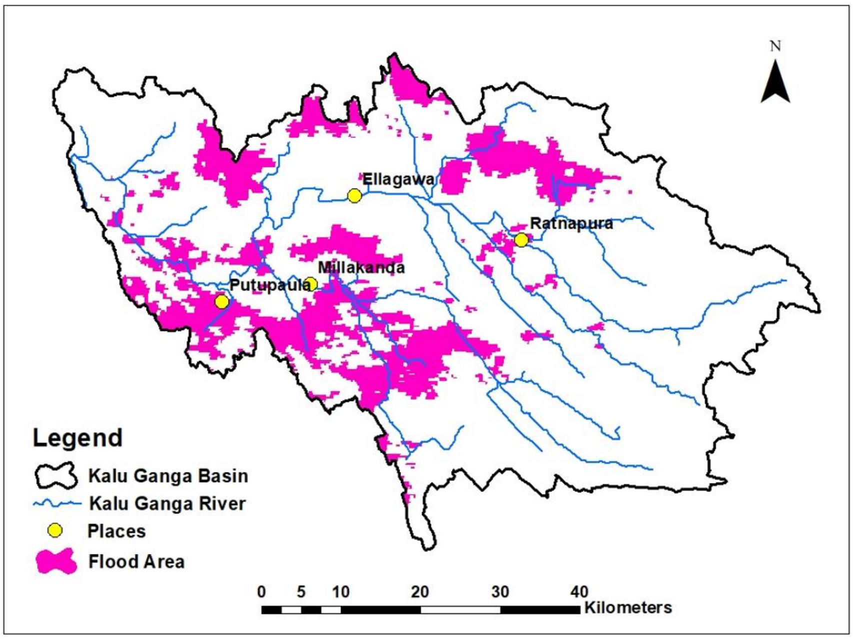


Figure 6-8: Flood Map – 5th September 2005 (MODIS)

The flood areas from the MODIS image and RRI model do not match along the river from Ratnapura to the Ellagawa site, below the Ellagawa site, and far west which is the Kalutara site. The flood areas on the top north side of the MODIS image are also not correct because there will be no flood on the high mountainous side. The event of September 2005 has a return period of 3 years.

**Flood Map - 29th April 2011**

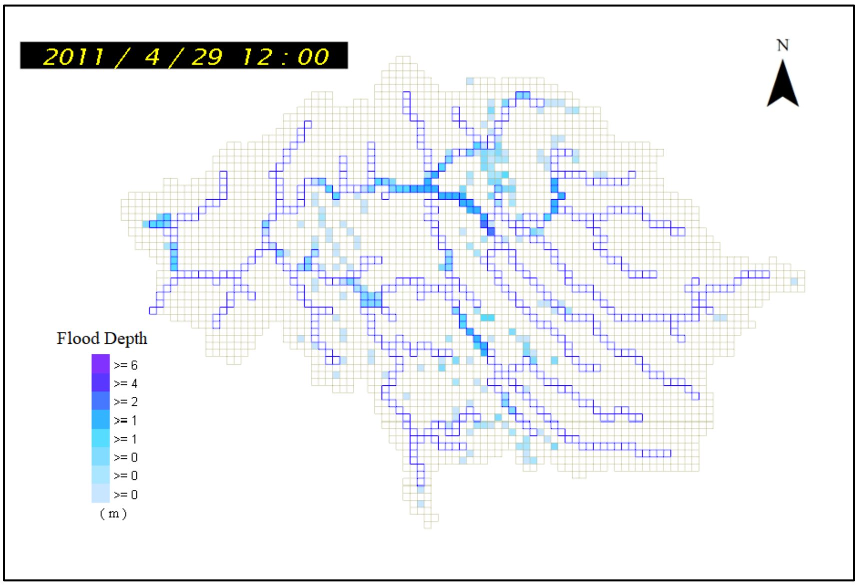


Figure 6-9: Flood Inundation Map – 29th April 2011 (RRI Model)

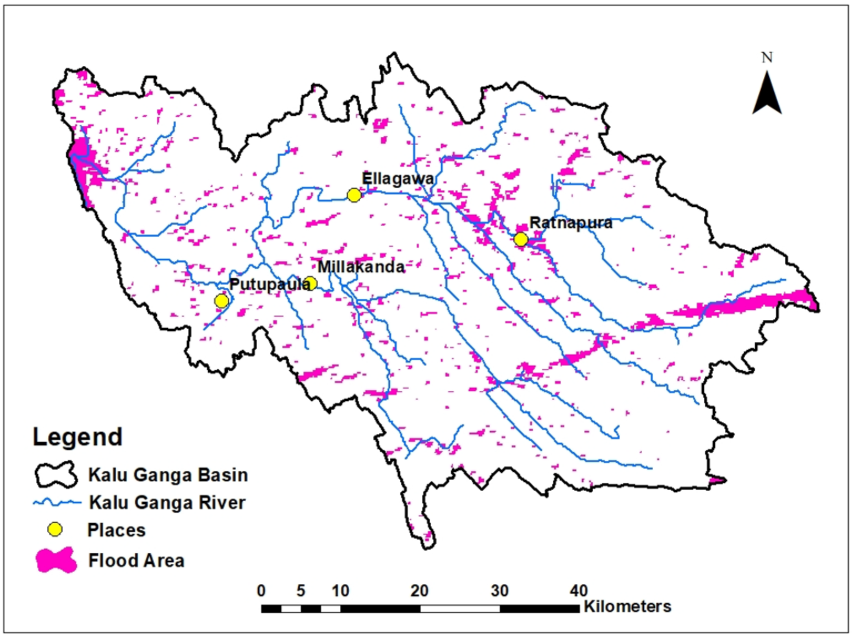


Figure 6-10: Flood Map – 29th April 2011 (MODIS)

The flood areas from the MODIS image at the eastern side are not correct since the flood areas are perpendicular to the river. The flood areas from the MODIS image and RRI model matches in Ratnapura site and the far west which is the Kalutara flood area. The event of April 2011 has a return period of 2 years.

**Flood Map - 19th May 2013**

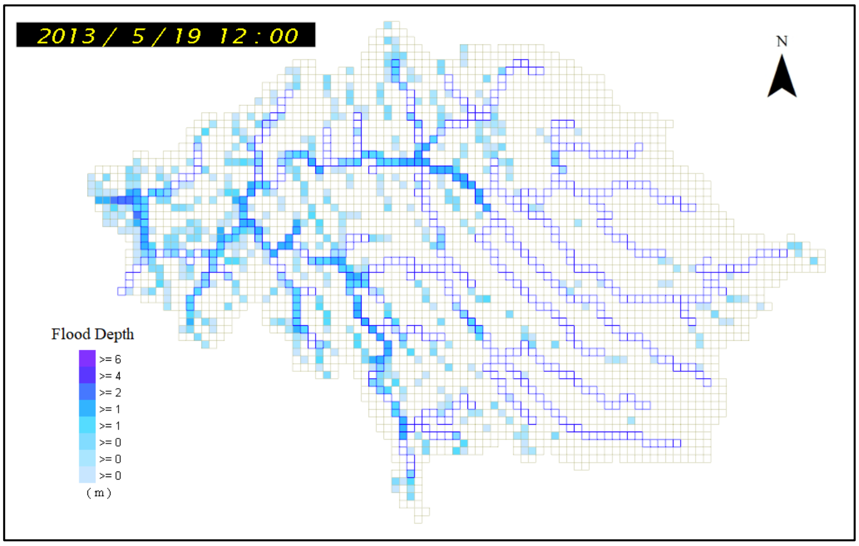


Figure 6-11: Flood Inundation Map – 19th May 2013 (RRI Model)

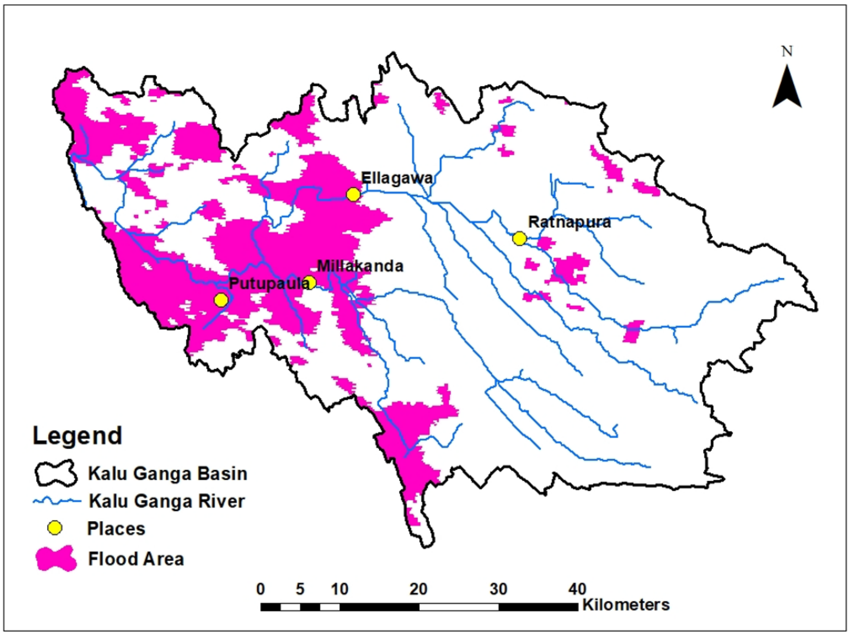


Figure 6-12: Flood Map – 19th May 2013 (MODIS)

The flood areas from the MODIS image and RRI model do not match along the river from Ratnapura to the Ellagawa site. The flood areas on the bottom south side of the MODIS image are also not correct because there will be no flood on the high mountainous side. The event of May 2013 has a return period of 3 years.

## 6.3 Flood Areas from AHP Method and RRI Model

Table 6-1 shows the flood area in square kilometers and percentage of the various categories of flood susceptibility map obtained from the AHP method in ArcMap and the event-based flood inundation map with flood depth obtained from the RRI model.

Table 6-1: Flood Areas from AHP Method and RRI Model

| Sl. No. | Description | Flood Area | |
|---|---|---|---|
| | | Area ($km^2$) | Area (%) |
| 1. | AHP (ArcMap) | | |
| | (i) Very High | 267 | 8.4 |
| | (ii) High and above | 1,149 | 36 |
| | (iii) Medium and above | 1,278 | 40.1 |
| 2. | RRI Model (May 2003) | | |
| | (i) Flood depth ≥ 1 m | 217.9 | 6.3 |
| | (ii) Flood depth ≥ 2 m | 129.6 | 3.7 |
| | (iii) Flood depth ≥ 4 m | 30 | 0.9 |
| 3. | RRI Model (April 2008) | | |
| | (i) Flood depth ≥ 1 m | 193.6 | 5.6 |
| | (ii) Flood depth ≥ 2 m | 124.7 | 3.6 |
| | (iii) Flood depth ≥ 4 m | 28.4 | 0.8 |
| 4. | RRI Model (May 2008) | | |
| | (i) Flood depth ≥ 1 m | 108.5 | 3.1 |
| | (ii) Flood depth ≥ 2 m | 39.7 | 1.1 |
| | (iii) Flood depth ≥ 4 m | 6.5 | 0.2 |

The Very High category in the flood susceptibility map is the most probable flood occurrence area. The Flood Susceptibility Map obtained from the AHP method in ArcMap shows a flood susceptibility area of 267 $km^2$ (8.4%) under the Very High category.

The flood depths greater than or equivalent to 1 meter cover all the flood depths. The flood inundation area of May 2003, April 2008, and May 2009 events with flood depths greater or equivalent to 1 meter are as follows:

- The flood inundation map of May 2003 obtained from the RRI Model has an inundation area of 217.9 $km^2$ (6.3%) with flood depths greater than or equivalent to 1 meter.
- The flood inundation map of April 2008 obtained from the RRI Model has an inundation area of 193.6 $km^2$ (5.6%) with flood depths greater than or equivalent to 1 meter.
- The flood inundation map of May 2008 obtained from the RRI Model has an inundation area of 108.5 $km^2$ (3.1%) with flood depths greater than or equivalent to 1 meter.

The flood susceptibility map from the AHP method has a higher area than the flood inundation map from the RRI model and this is because the simulated or observed flood maps are always a subset of the flood susceptibility map.

# CHAPTER 7

## 7 DISCUSSION

The flood susceptibility area obtained from AHP cannot be directly compared with the flood inundation map obtained from the RRI model because the flood susceptibility area from AHP is not a flood map with a particular return period but an area with different potentials for flooding.

### 7.1 Analytical Hierarchy Process (AHP)

In the AHP method, the rainfall parameter taken from observed rainfall data greatly influences the flood susceptibility map. The flood susceptibility map will also be influenced by the number of parameters and weights taken for the analysis. The minimum number of parameters taken in the AHP method should be three (Saaty, 1987).

In the flood susceptibility area obtained from AHP, the flood probability category with Very High, the lower will be the return period, and higher will be the return period as the flood probability category decreases to Low flood probability category.

Swain et al. (2020) used remote sensing and AHP-GIS technique to obtain the flood susceptibility zones in Bihar, India. A total of 21 criteria [(a) river network density, (b) Precipitation, (c) elevation, (d) SPI, (e) profile curvature, (f) slope, (g) ruggedness index, (h) distance from river, (i) landforms, (j) soil moisture, (k) soil type, (l) soil erodibility factor, (m) TWI, (n) LU/LC, (o) rainfall erosivity factor, (p) NDVI, (q) SAVI, (r) GMIS, (s) population density, (t) distance to road network, and (u) HBSE] grouped into five (5) primary criteria [(a) morphometric, (b) hydrologic, (c) anthropogenic, (d) permeability, and (e) land cover dynamics] were used. An area of 40.36% was in the High to Very High flood susceptibility category that was in the vicinity of rivers. In this research, the area concentrated in the High to Very High flood susceptibility category was 36% and the food occurring in the vicinity of rivers show a similar pattern.

Rimba et al. (2017) carried out a study in Okazaki City, Aichi Prefecture, Japan to study the area that was vulnerable to flooding using GIS, remote sensing, and spatial multi-criteria evaluation with the Analytical Hierarchy Process (AHP) approach. Five (5) parameters (drainage density, slope, infiltration rate, land cover, and rainfall intensity) were used in the study. A total area of 11.1% was found in the Very Highly vulnerable category to flooding. In this research, the area under the Very High category was 8.4%.

Das (2018) carried out a study in the Vaitarna river basin, Maharashtra, India to demarcate flood susceptible regions by using the Analytical Hierarchy Process (AHP) and geospatial techniques that gave a cost-effective and less time-consuming analysis. Nine (9) parameters (slope, elevation, rainfall, distance from the river, land use, flow accumulation, geology, curvature map, and TWI) were used in the study. A total area of 20% was found in the Very High probability of flood category. In this research, it was 8.4%.

Hammami et al. (2019) carried out a study for the examination of flood susceptibility in the city of Tunis using Analytical Hierarchy Process (AHP) and Geographical Information System (ArcGIS). Eight (8) parameters (elevation, land use/land cover, lithology, slope, rainfall, drainage density, groundwater level, and soil) were used in the study. A total area of 51.06% was found in the Very High probability of flood category. In this research, it was 8.4%.

## 7.2 Rainfall-Runoff-Inundation (RRI) Model

The built-in grided data with *nr* river value and *ns* slope values highly influence the flood inundation map. The most significant parameters in the RRI model are channel (*nr* river) and hillslope roughness coefficient (*ns* slope) (Abdel et al., 2018). In the RRI model, it was observed that the flood inundation area mostly took place along the length of the river.

MODIS images were used to validate the flood inundation maps with the RRI model. All the MODIS image shows flood areas in some areas where it should not be flooding, and this is due to the errors in processing satellite images. The MODIS image also neglects the permanent water bodies whereby in some river path where it should be flooding is not shown (Onjira & Sayama, 2014).

Rasmy et al. (2019) carried out a study in the Kalu river basin, Sri Lanka using the Water and Energy Budget-based Rainfall-Runoff-Inundation (WEB-RRI) model, by combining the RRI model's diffusive wave flow equations into a land surface model (hydro-SiB2) to include water and energy budget processes, soil moisture dynamics, land-vegetation-atmosphere interactions, and 2-D lateral water flows to improve evapotranspiration (ET), interception, runoff, soil moisture, and inundation processes. Satellite data were used for obtaining the inundation areas using the WER-RRI model and it shows inundation areas in the extreme hilly areas. Whereas, in this study, inbuilt gridded data were used as it was not possible to use the satellite data in the RRI model. The processing power of the normal computer is not adequate to handle the satellite data covering a huge study area of the Kalu Ganga basin (3,191 $km^2$) as input in the RRI model. In this case study, the RRI model shows the inundation areas in the extreme hilly areas which match with the WEB-RRI model.

San et al. (2020) carried out a study in the Bago river basin, Myanmar using RRI and SOBEK models to develop a flood inundation map. In comparison, the SOBEK model has higher accuracy than the RRI model. Nonetheless, when the calculation time and cost are considered, the RRI model is preferred, as it is faster and easily available.

# CHAPTER 8

## 8 CONCLUSIONS

- A flood susceptibility map was obtained using the AHP method in ArcMap and flood inundation maps of May 2003, April 2008, and May 2008 were obtained in the RRI model.
- Six flood influencing parameters (elevation, slope, rainfall, flow accumulation, land use, and soil) were taken for obtaining a flood susceptibility map in the AHP method. In the AHP method, the rainfall parameter greatly influenced the flood susceptibility map. The flood susceptibility map has a flood susceptibility area under the Very High category of 267 km² (8.4%) in the Kalu Ganga basin which is the most probable flood occurrence area.
- In the RRI model, the built-in data (Flow Direction, Flow Accumulation, DEM, Soil, and Land Cover) with observed rainfall data was used for generating flood inundation maps. The built-in data with *nr* river and *ns* slope values greatly influence the flood inundation map in the RRI model. The flood inundation maps of May 2003, April 2008, and May 2008 have an area of 217.9 km² (6.3%), 193.6 km² (5.6%), and 108.5 km² (3.1%), respectively with flood depths greater than or equivalent to 1 meter in Kalu Ganga basin where the flood depths greater than or equivalent to 1 meter cover all the flood depths.
- The flood susceptibility map obtained using the AHP method in ArcMap has a higher flood area than the flood inundation map obtained from the RRI model. The flood susceptibility map obtained from the AHP method in ArcMap is a flood probability map and the flood inundation map from the RRI model is a modeling flood map. Therefore, they are different. But the flood inundation area occurs within the flood susceptibility map.

# CHAPTER 9

## 9 RECOMMENDATIONS

In the AHP method, the rainfall parameter taken from observed rainfall data greatly influences the flood susceptibility map. The narrow gap or the bottleneck in the Ellagawa area of the river retains the water for many days in the Ratnapura area before it discharges to the Kalutara area. Rainfall in the Rathnapura area can flood the Kalutara area and those cannot be considered in AHP. For further study, additional parameters or different parameters can be taken with different weights to analyze the flood susceptibility behavior in the Kalu Ganga basin. Parameters like Topographic Wetness Index (TWI), Curvature, Geology, and distance from the river can be used to analyze the flood probability area (Das, 2018).

In the RRI model, built-in grided data was taken for the study. For future study, Satellite data (DEM, Flow Accumulation, and Flow Direction) can be taken to analyze smaller areas (catchment/floodplain areas) in the Kalu Ganga basin.

# BIBLIOGRAPHY

Abdel, F. M., Kantoush, S. A., Saber, M., & Sumi, T. (2018). Rainfall-Runoff modeling for extreme flash floods in Wadi Samail, Oman. *Journal of Japan Society of Civil Engineers, Ser. B1 (Hydraulic Engineering)*, *74*(5), I_691-I_696. https://doi.org/10.2208/JSCEJHE.74.5_I_691

Acharya, N., & Singh, S. (2018). An IWD-based feature selection method for intrusion detection system. *Soft Computing*, *22*(13), 4407–4416. https://doi.org/10.1007/S00500-017-2635-2

Ampitiyawatta, A., & Guo, S. (2010). Precipitation trends in the Kalu Ganga basin in Sri Lanka. *Journal of Agricultural Sciences*, *4*(1), 10. https://doi.org/10.4038/JAS.V4I1.1641

Arcement, G. J., Schneider, V. R., & U.S. G.P.O. ; For sale by the Books and Open-File Reports Section, U. S. G. S. (1989). Guide for selecting Manning's roughness coefficients for natural channels and flood plains. In *Water Supply Paper*. https://doi.org/10.3133/wsp2339

Bernasconi, M., Choirat, C., & Seri, R. (2009). The Analytic Hierarchy Process and the Theory of Measurement. *University of Venice "Ca'' Foscari", Department of Economics, Working Papers," 56*. https://doi.org/10.2307/27784145

Bhagabati, S. S., & Kawasaki, A. (2017). Consideration of the rainfall-runoff-inundation (RRI) model for flood mapping in a deltaic area of myanmar. *Hydrological Research Letters*, *11*(3), 155–160. https://doi.org/10.3178/HRL.11.155

Das, S. (2018). Geographic information system and AHP-based flood hazard zonation of Vaitarna basin, Maharashtra, India. *Arabian Journal of Geosciences*, *11*(19). https://doi.org/10.1007/S12517-018-3933-4

Hammami, S., Zouhri, L., Souissi, D., Souei, A., Zghibi, A., Marzougui, A., & Dlala, M. (2019). Application of the GIS based multi-criteria decision analysis and analytical hierarchy process (AHP) in the flood susceptibility mapping (Tunisia). *Arabian Journal of Geosciences 2019 12:21*, *12*(21), 1–16. https://doi.org/10.1007/S12517-019-4754-9

Hapuarachchi, H. A. P., Wang, Q. J., & Pagano, T. C. (2011). A review of advances in flash flood forecasting. *Hydrological Processes*, *25*(18), 2771–2784. https://doi.org/10.1002/HYP.8040

JICA. (2009). *Comprehensive study on disaster management in Sri Lanka, Final Report (Supporting Report), Asian Disaster Reduction Center, Ministry of Disaster Management and Human Rights, Department of Irrigation of the Ministry of Irrigation and Water Management.*

Khaing, Z. M., Zhang, K., Sawano, H., Shrestha, B. B., Sayama, T., & Nakamura, K. (2019). Flood hazard mapping and assessment in data-scarce Nyaungdon area, Myanmar. *PLoS ONE*, *14*(11). https://doi.org/10.1371/JOURNAL.PONE.0224558

Moriasi, D. N., Gitau, M. W., Pai, N., & Daggupati, P. (2015). Hydrologic and water quality models: Performance measures and evaluation criteria. *Transactions of the ASABE*, *58*(6), 1763–1785. https://doi.org/10.13031/TRANS.58.10715

Onjira, P. P. I., & Sayama, T. (2014). *Application of remote sensing and Rainfall-Runoff-Inundation model to near realtime flood inundation mapping in Kenya.*

Ouma, Y. O., & Tateishi, R. (2014). Urban Flood Vulnerability and Risk Mapping Using Integrated Multi-Parametric AHP and GIS: Methodological Overview and Case Study Assessment. *Water 2014, Vol. 6, Pages 1515-1545*, *6*(6), 1515–1545. https://doi.org/10.3390/W6061515

PDNA. (2017). *Sri Lanka Rapid Post Disaster Needs Assessment Floods and Landslides*.

Peiris, T., Nandalal, H., Samarasinghe, J., & Fowze, J. S. M. (2009). *Flood Risk Analysis at Kalu-Ganga River basin in Sri Lanka*.

Rabunal, J. R., Dorado, J., & Pazos Sierra, Alejandro. (2009). *Encyclopedia of artificial intelligence*. 17.

Rasmy, M., Sayama, T., & Koike, T. (2019). Development of water and energy Budget-based Rainfall-Runoff-Inundation model (WEB-RRI) and its verification in the Kalu and Mundeni River Basins, Sri Lanka. *Journal of Hydrology*, *579*, 124163. https://doi.org/10.1016/J.JHYDROL.2019.124163

Rimba, A., Setiawati, M., Sambah, A., & Miura, F. (2017). Physical Flood Vulnerability Mapping Applying Geospatial Techniques in Okazaki City, Aichi Prefecture, Japan. *Urban Science*, *1*(1), 7. https://doi.org/10.3390/URBANSCI1010007

Saaty. (1977). A scaling method for priorities in hierarchical structures. *Journal of Mathematical Psychology*, *15*(3), 234–281. https://doi.org/10.1016/0022-2496(77)90033-5

Saaty. (1980). The analytic hierarchy process: Planning, priority setting, resource allocation: Thomas L. SAATY McGraw-Hill, New York, 1980, xiii. In *European Journal of Operational Research* (Vol. 9, Issue 1). McGraw-Hill.

Saaty. (1987). The analytic hierarchy process-what it is and how it is used. *Mathematical Modelling*, *9*(3–5), 161–176. https://doi.org/10.1016/0270-0255(87)90473-8

Saaty, T. L. (1990). How to make a decision: The analytic hierarchy process. *European Journal of Operational Research*, *48*(1), 9–26. https://doi.org/10.1016/0377-2217(90)90057-I

San, Z. M. L. T., Zin, W. W., Kawasaki, A., Acierto, R. A., & Oo, T. Z. (2020). Developing flood inundation map using RRI and SOBEK models: A case study of the Bago River Basin, Myanmar. *Journal of Disaster Research*, *15*(3), 277–287. https://doi.org/10.20965/JDR.2020.P0277

Sayama, T., Ozawa, G., Kawakami, T., Nabesaka, S., & Fukami, K. (2012). Rainfall–runoff–inundation analysis of the 2010 Pakistan flood in the Kabul River basin.

*Https://Doi.Org/10.1080/02626667.2011.644245*, *57*(2), 298–312. https://doi.org/10.1080/02626667.2011.644245

Subramany, K. (2019). *Engineering Hydorlogy*.

Swain, K. C., Singha, C., & Nayak, L. (2020). Flood Susceptibility Mapping through the GIS-AHP Technique Using the Cloud. *ISPRS International Journal of Geo-Information 2020, Vol. 9, Page 720*, *9*(12), 720. https://doi.org/10.3390/IJGI9120720

TAHAL Group. (2013). *Pre-Feasibility Study of Kalu Ganga Basin*.

Triantaphyllou, E., & Mann, S. (1995). Using the analytic hierarchy process for decision making in engineering applications: Some challenges. *The International Journal of Industrial Engineering: Theory, Applications and Practice*, *2*, 35–44.

# ANNEXURE 1

## DOUBLE MASS CURVE AFTER FILLING THE MISSING RAINFALL DATA

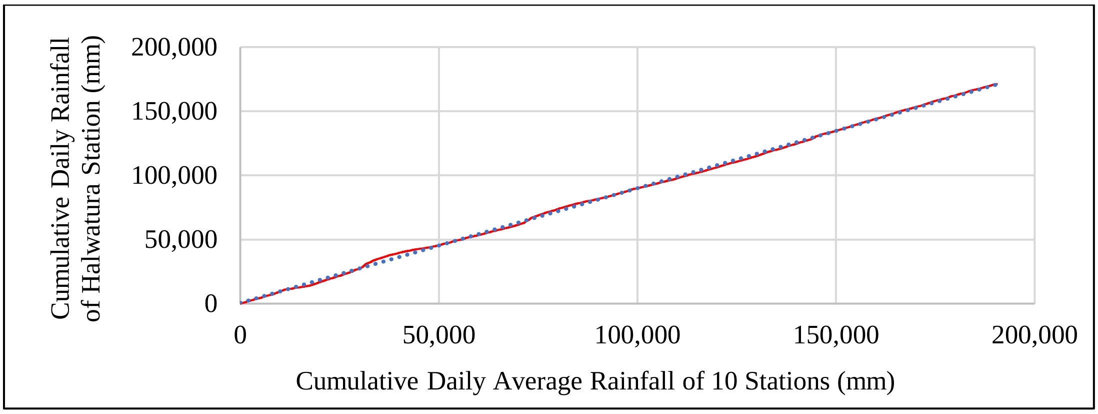


Figure A.1.1 Double Mass Curve – Halwatura

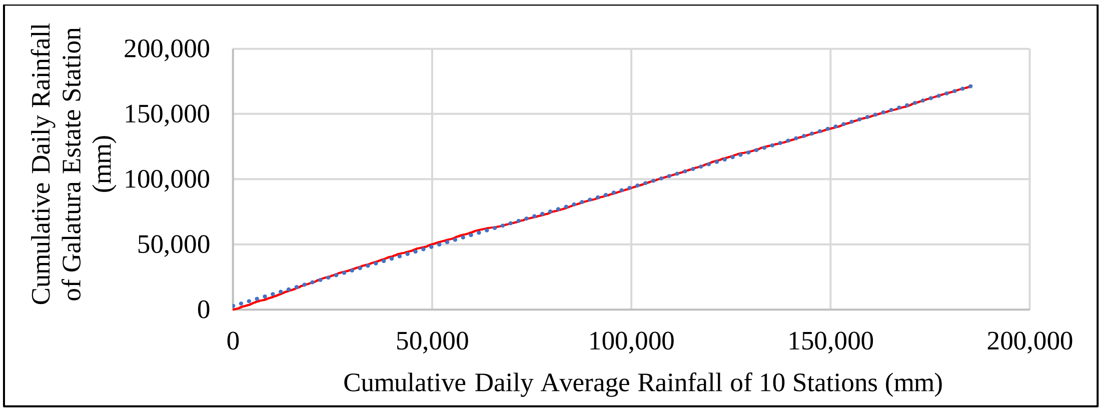


Figure A.1.2 Double Mass Curve – Galatura Estate

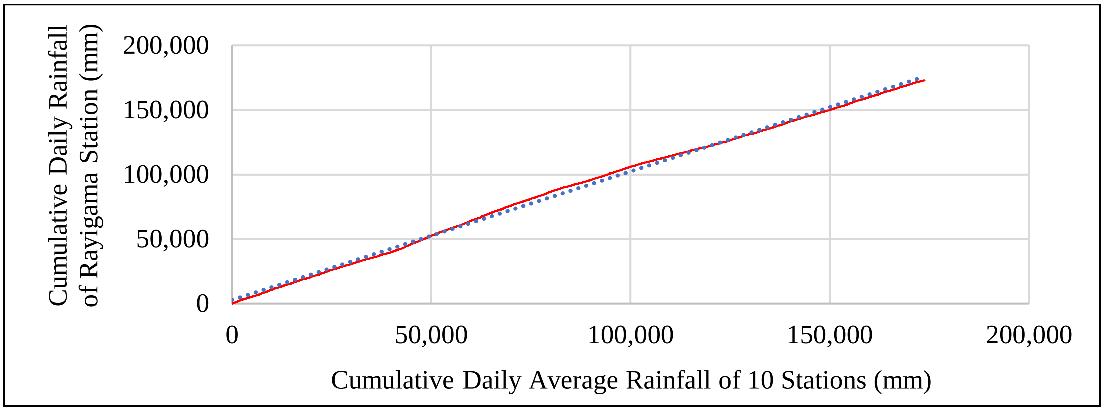


Figure A.1.3 Double Mass Curve – Rayigama

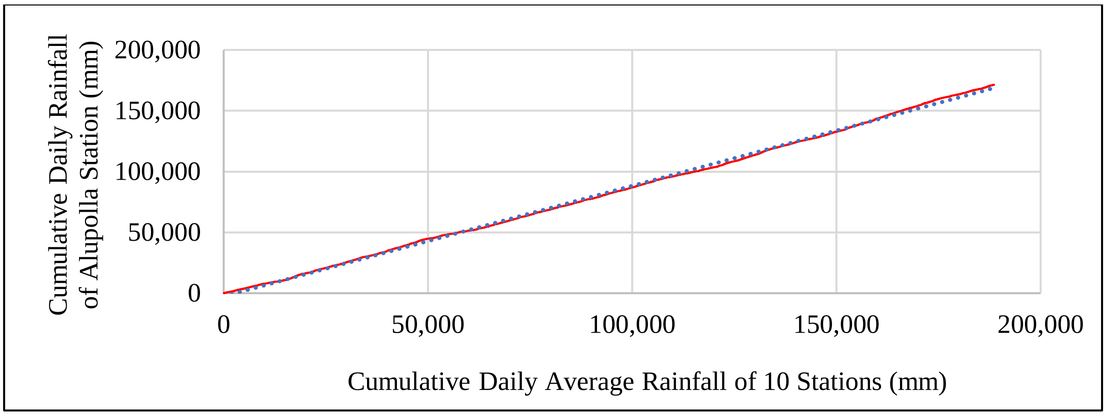


Figure A.1.4 Double Mass Curve – Alupolla

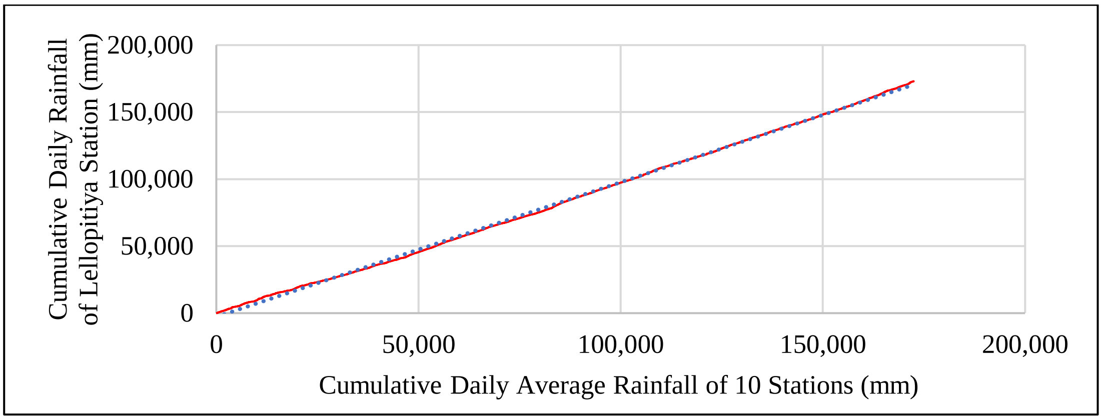


Figure A.1.5 Double Mass Curve – Lellopitiya

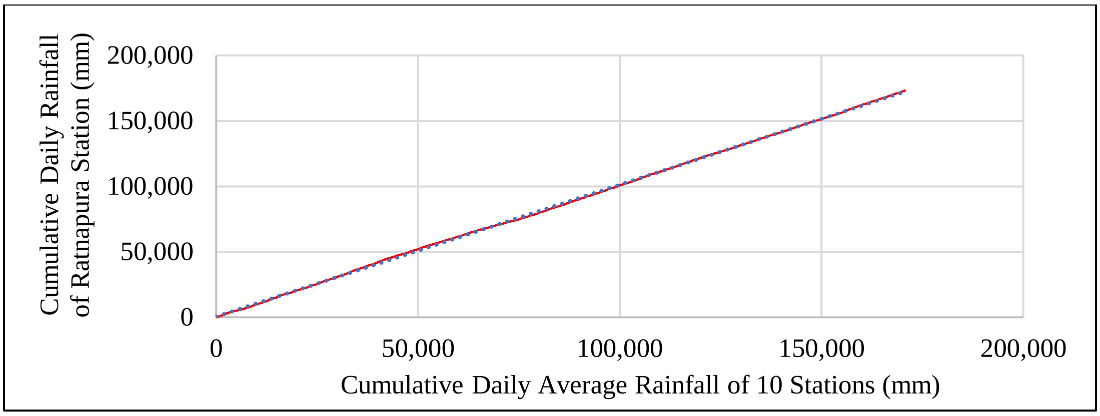


Figure A.1.6 Double Mass Curve – Ratnapura

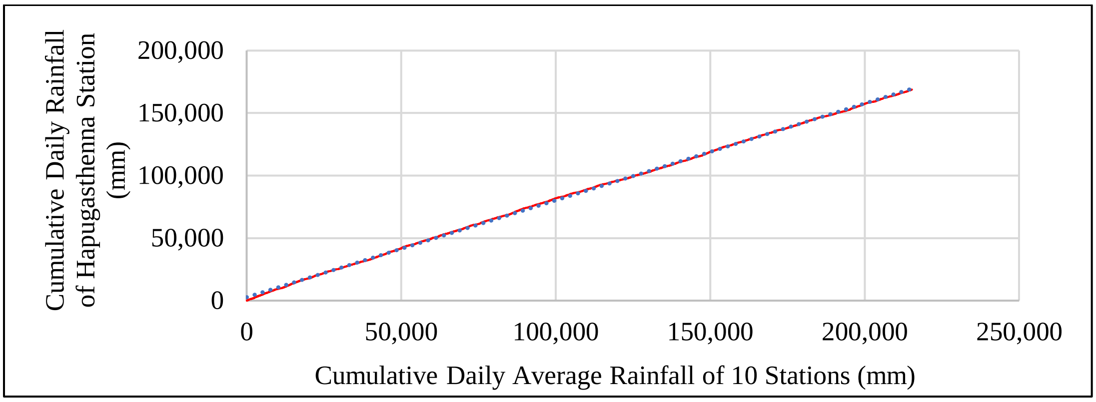


Figure A.1.7 Double Mass Curve – Hapugasthenna

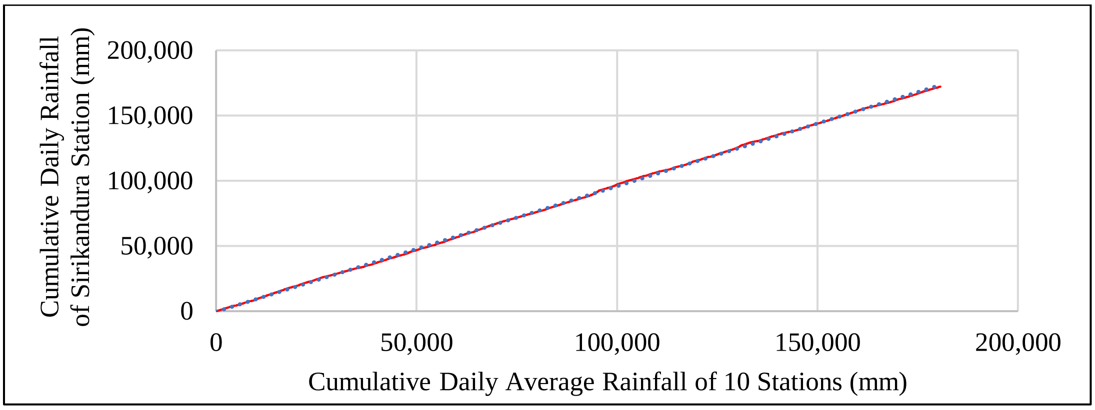


Figure A.1.8 Double Mass Curve – Sirikandura

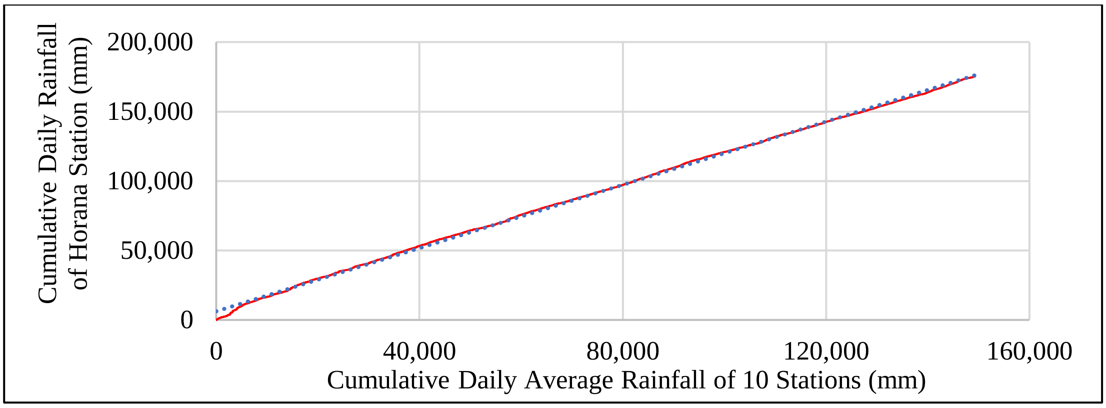


Figure A.1.9 Double Mass Curve – Horana

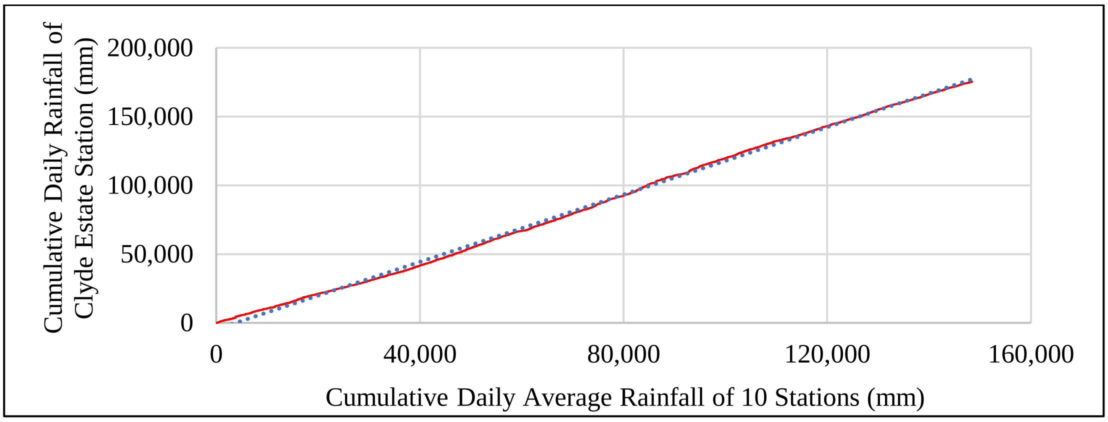


Figure A.1.10 Double Mass Curve – Clyde Estate

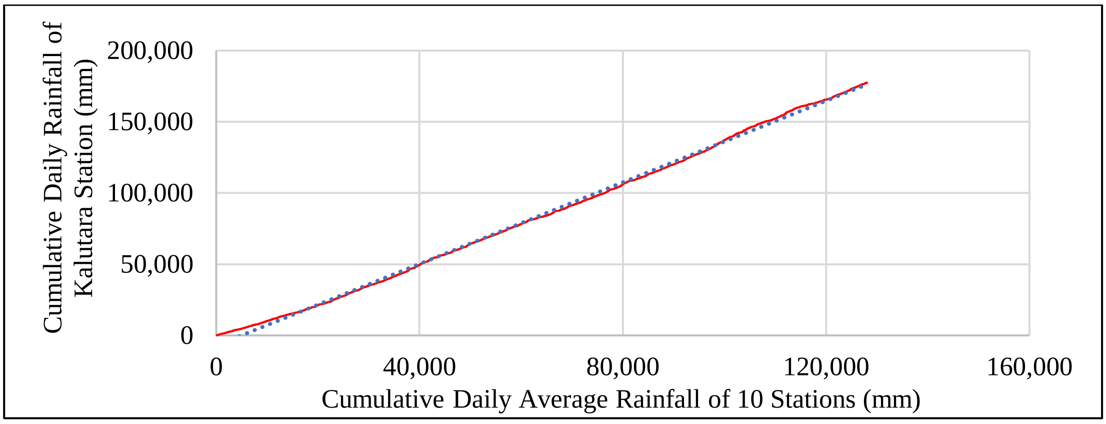


Figure A.1.11 Double Mass Curve – Kalutara

# ANNEXURE 2

## STREAMFLOW VERSUS RAINFALL AFTER FILLING THE MISSING DATA

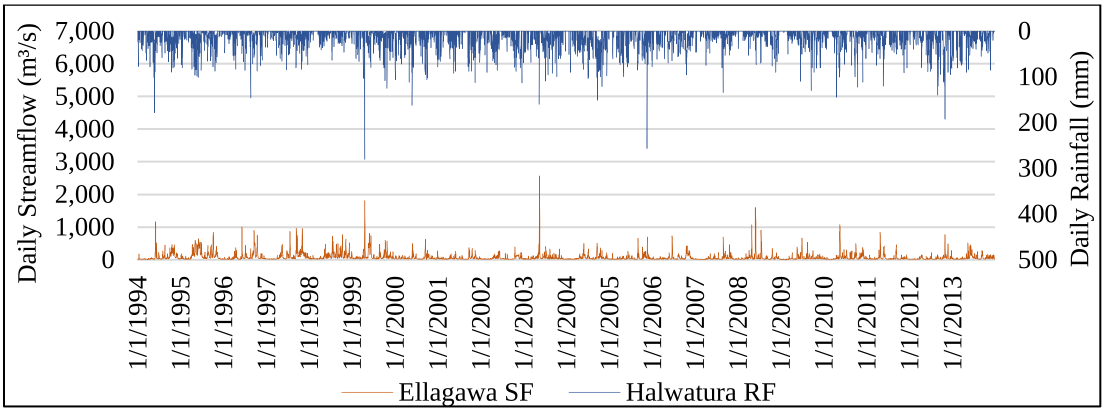


Figure A.2.1 Ellagawa streamflow versus Halwatura rainfall

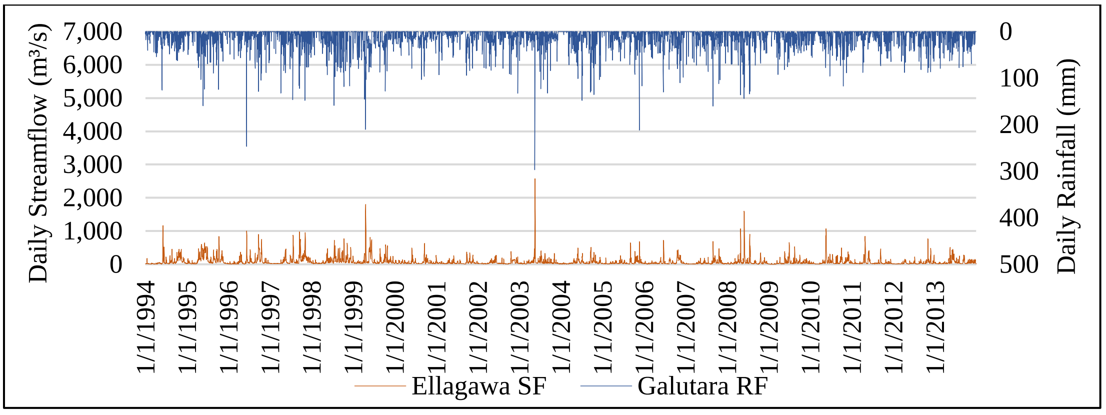


Figure A.2.2 Ellagawa streamflow versus Galutara Estate rainfall

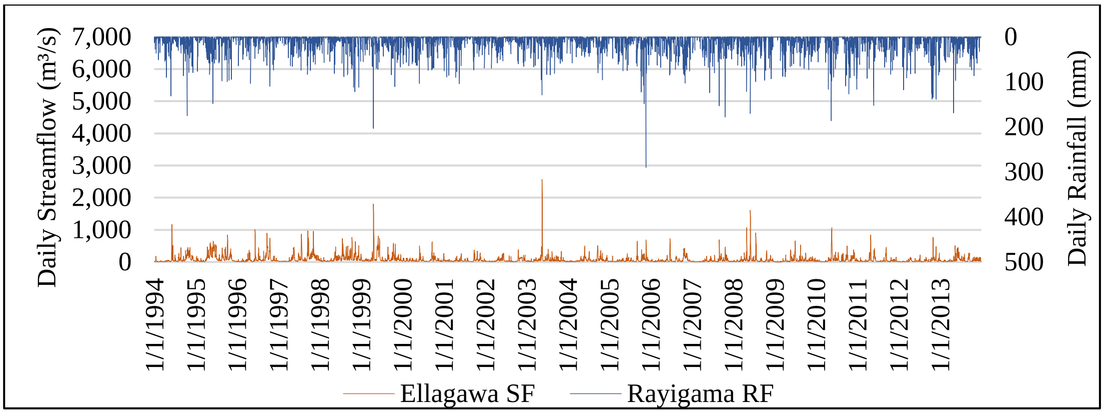


Figure A.2.3 Ellagawa streamflow versus Rayigama rainfall

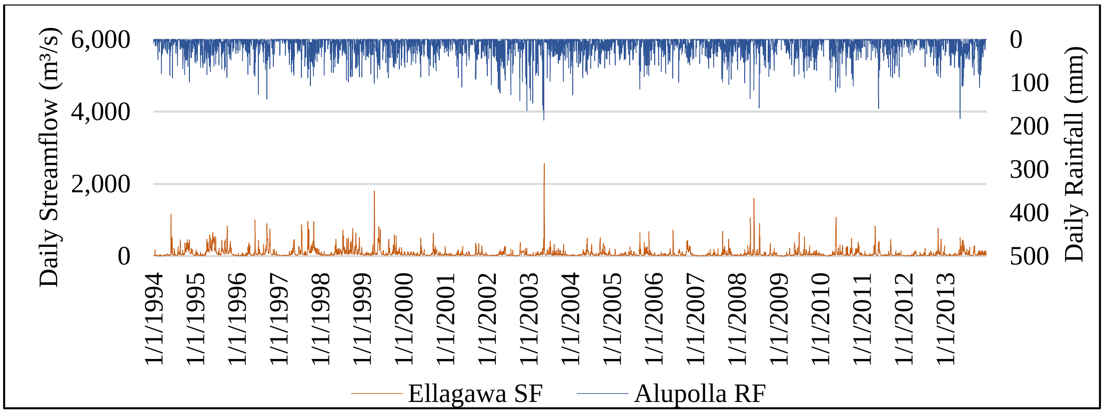


Figure A.2.4 Ellagawa streamflow versus Alupolla rainfall

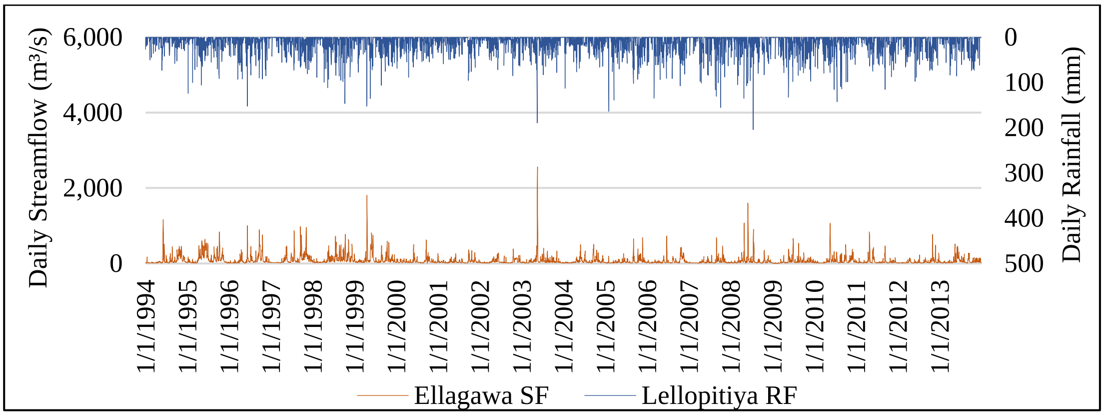


Figure A.2.5 Ellagawa streamflow versus Lellopitiya rainfall

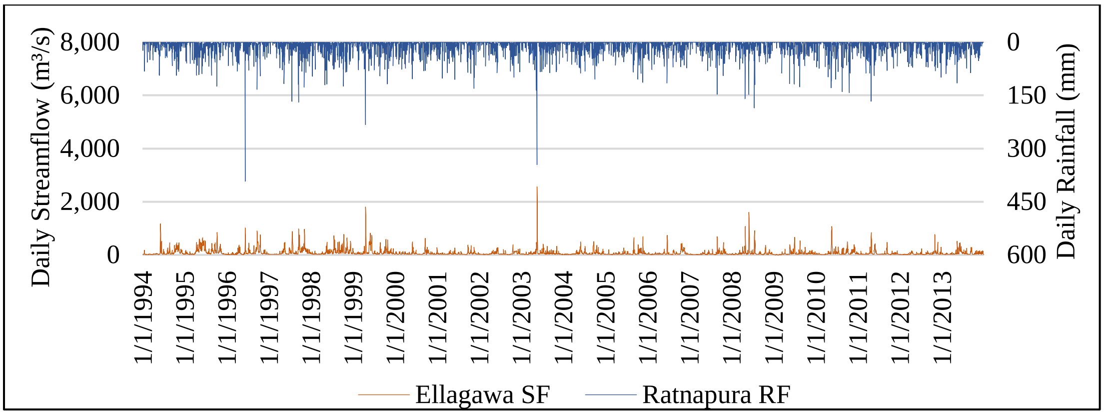


Figure A.2.6 Ellagawa streamflow versus Ratnapura rainfall

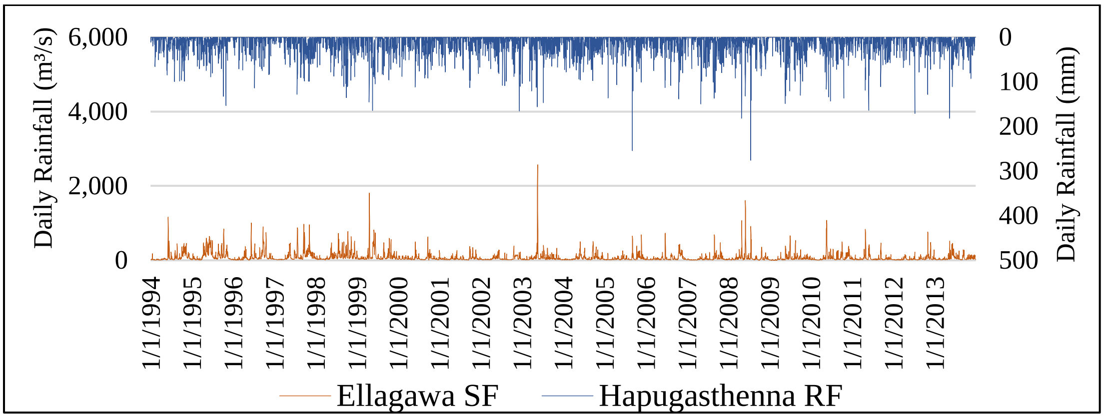


Figure A.2.7 Ellagawa streamflow versus Hapugasthenna rainfall

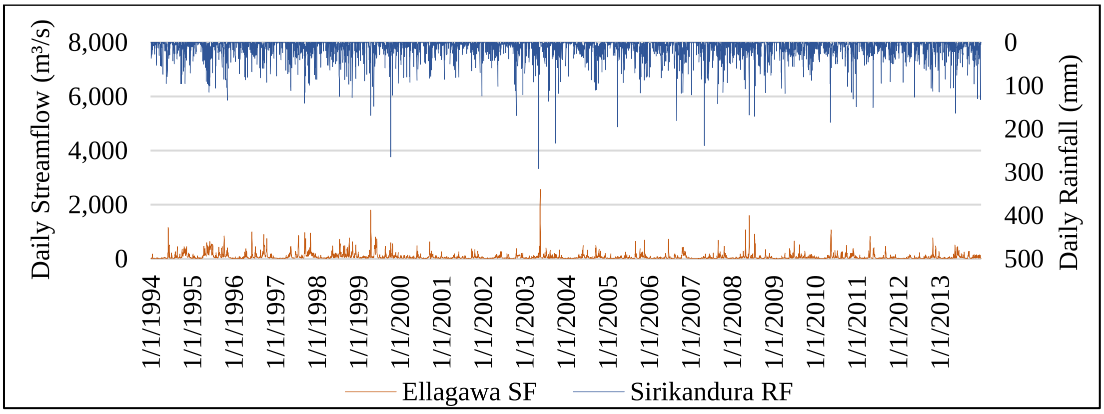


Figure A.2.8 Ellagawa streamflow versus Sirikandura rainfall

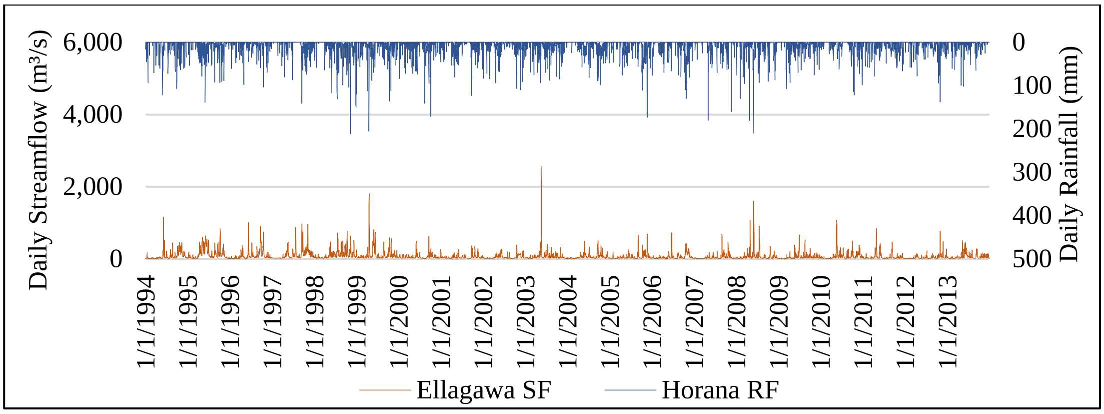


Figure A.2.9 Ellagawa streamflow versus Horana rainfall

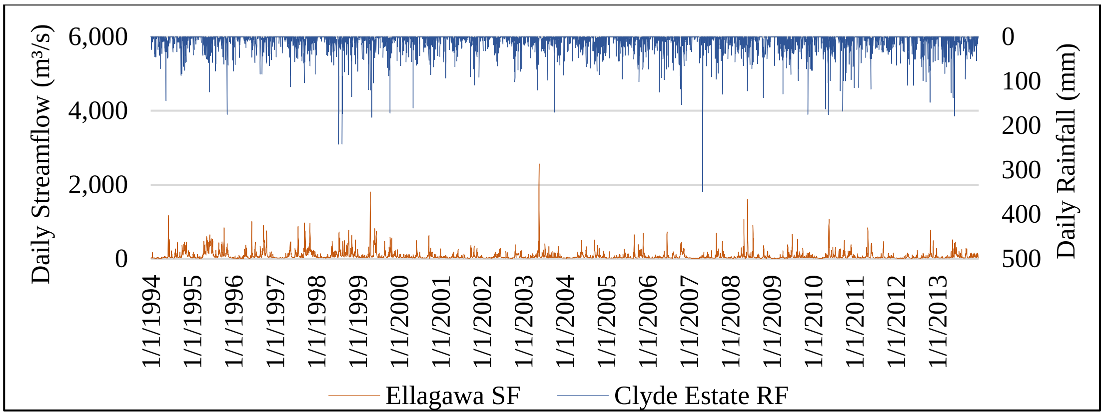


Figure A.2.10 Ellagawa streamflow versus Clyde Estate rainfall

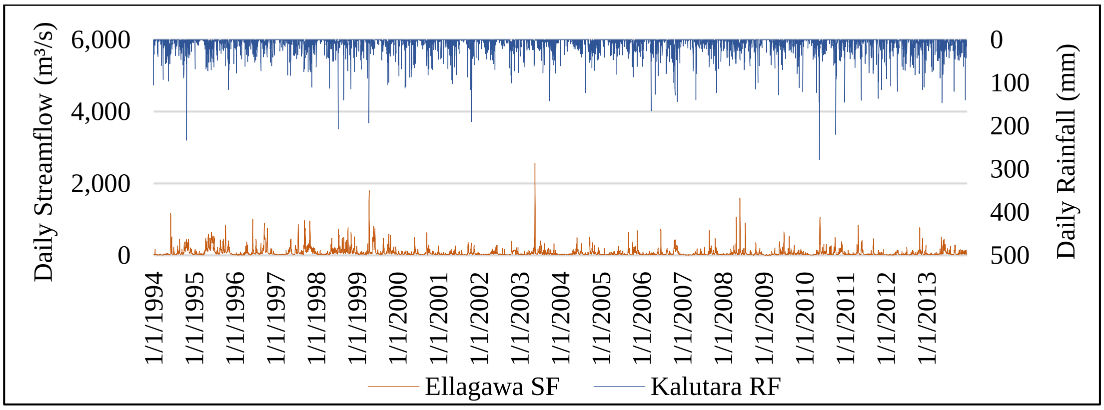


Figure A.2.11 Ellagawa streamflow versus Kalutara rainfall

# ANNEXURE 3

## PAIRWISE COMPARISON MATRIX AND SCORE OF SUBCATEGORIES

Table A.3.1 Pairwise comparison matrix and score - Elevation

| Elevation (m) | > 681 | 471 - 680 | 271 - 470 | 121 - 270 | < 120 | Weight | Rank | CR |
|---|---|---|---|---|---|---|---|---|
| > 681 | 1 | 3 | 5 | 7 | 8 | 0.5 | 1 | |
| 471 - 680 | 1/3 | 1 | 3 | 5 | 6 | 0.26 | 2 | |
| 271 - 470 | 1/5 | 1/3 | 1 | 3 | 5 | 0.14 | 3 | 0.06 |
| 121 - 270 | 1/7 | 1/5 | 1/3 | 1 | 3 | 0.07 | 4 | |
| < 120 | 1/8 | 1/6 | 1/5 | 1/3 | 1 | 0.04 | 5 | |

Table A.3.2 Pairwise comparison matrix and score - Slope

| Slope (Degree) | > 24.1 | 15.1 - 24 | 8.66 - 15 | 3.66 - 8.65 | < 3.65 | Weight | Rank | CR |
|---|---|---|---|---|---|---|---|---|
| > 24.1 | 1 | 2 | 4 | 6 | 8 | 0.45 | 1 | |
| 15.1 - 24 | 1/2 | 1 | 3 | 5 | 7 | 0.3 | 2 | |
| 8.66 - 15 | 1/4 | 1/3 | 1 | 3 | 5 | 0.15 | 3 | 0.04 |
| 3.66 - 8.65 | 1/6 | 1/5 | 1/3 | 1 | 3 | 0.07 | 4 | |
| < 3.65 | 1/8 | 1/7 | 1/5 | 1/3 | 1 | 0.04 | 5 | |

Table A.3.3 Pairwise comparison matrix and score - Flow Accumulation

| Flow Accumulation | < 14,189 | 14,190 - 49,662 | 19,663 - 92,230 | 92,231 - 257,180 | > 257,181 | Weight | Rank | CR |
|---|---|---|---|---|---|---|---|---|
| < 14,189 | 1 | 2 | 4 | 6 | 8 | 0.46 | 1 | |
| 14,190 - 49,662 | 1/2 | 1 | 2 | 4 | 6 | 0.26 | 2 | |
| 19,663 - 92,230 | 1/4 | 1/2 | 1 | 2 | 5 | 0.15 | 3 | 0.04 |
| 92,231 - 25,7180 | 1/6 | 1/4 | 1/2 | 1 | 4 | 0.09 | 4 | |
| > 257,181 | 1/8 | 1/6 | 1/5 | 1/4 | 1 | 0.04 | 5 | |

Table A.3.4 Pairwise comparison matrix and score - Soil

| Soil | Brown Loams | Regosols | Podzolic Soils | Bog and Half-dog Soil | Alluvial Soil | Weight | Rank | CR |
|---|---|---|---|---|---|---|---|---|
| Brown Loams | 1 | 3 | 5 | 7 | 8 | 0.5 | 1 | |
| Regosols | 1/3 | 1 | 3 | 5 | 7 | 0.26 | 2 | |
| Podzolic Soils | 1/5 | 1/3 | 1 | 3 | 5 | 0.14 | 3 | 0.06 |
| Bog and Half-dog Soil | 1/7 | 1/5 | 1/3 | 1 | 3 | 0.07 | 4 | |
| Alluvial Soil | 1/8 | 1/7 | 1/5 | 1/3 | 1 | 0.04 | 5 | |

Table A.3.5 Pairwise comparison matrix and score - Land-use

| Land-use | Bare Land | Urban Areas | Forest | Agriculture | Water Bodies | Weight | Rank | CR |
|---|---|---|---|---|---|---|---|---|
| Bare Land | 1 | 2 | 3 | 4 | 5 | 0.42 | 1 | |
| Urban Areas | 1/2 | 1 | 2 | 3 | 4 | 0.26 | 2 | |
| Forest | 1/3 | 1/2 | 1 | 2 | 3 | 0.16 | 3 | 0.02 |
| Agriculture | 1/4 | 1/3 | 1/2 | 1 | 2 | 0.1 | 4 | |
| Water Bodies | 1/5 | 1/4 | 1/3 | 1/2 | 1 | 0.06 | 5 | |

Table A.3.6 Pairwise comparison matrix and score - Rainfall

| Rainfall (mm) | < 3479 | 3479 - 3669 | 3669 - 3757 | 3757 - 3845 | > 3845 | Weight | Rank | CR |
|---|---|---|---|---|---|---|---|---|
| < 3479 | 1 | 3 | 5 | 7 | 9 | 0.49 | 1 | |
| 3479 - 3669 | 1/3 | 1 | 3 | 7 | 9 | 0.29 | 2 | |
| 3669 - 3757 | 1/5 | 1/3 | 1 | 3 | 5 | 0.13 | 3 | 0.06 |
| 3757 - 3845 | 1/7 | 1/7 | 1/3 | 1 | 3 | 0.06 | 4 | |
| > 3845 | 1/9 | 1/9 | 1/5 | 1/3 | 1 | 0.03 | 5 | |